



Universidade de Brasília – UnB
Instituto de Geociências – IG
Programa de Pós-Graduação em Geologia

**APLICAÇÃO DE TÉCNICAS DE ANÁLISE ESTATÍSTICA
MULTIVARIADA E MACHINE LEARNING PARA O
MAPEAMENTO DO FOOTPRINT GEOQUÍMICO DA
MINERALIZAÇÃO DE OURO NO DISTRITO MINEIRO
DE JACOBINA**

APPLICATION OF MULTIVARIATE STATISTICAL ANALYSIS AND
MACHINE LEARNING TECHNIQUES FOR MAPPING THE
GEOCHEMICAL FOOTPRINT OF GOLD MINERALIZATION IN THE
JACOBINA MINING DISTRICT

BEATRIZ DANTAS RABELO DE ALMEIDA

DISSERTAÇÃO DE MESTRADO n°525

Orientadora: Prof. Dra. Catarina Laboure Bemfica Toledo

Co-orientadora: Profa. Dra. Adalene Moreira Silva

Brasília

2024

BEATRIZ DANTAS RABELO DE ALMEIDA

**APLICAÇÃO DE TÉCNICAS DE ANÁLISE ESTATÍSTICA
MULTIVARIADA E MACHINE LEARNING PARA O
MAPEAMENTO DO FOOTPRINT GEOQUÍMICO DA
MINERALIZAÇÃO DE OURO NO DISTRITO MINEIRO
DE JACOBINA**

APPLICATION OF MULTIVARIATE STATISTICAL ANALYSIS AND
MACHINE LEARNING TECHNIQUES FOR MAPPING THE
GEOCHEMICAL FOOTPRINT OF GOLD MINERALIZATION IN THE
JACOBINA MINING DISTRICT

Dissertação de mestrado apresentada
ao curso de Pós-Graduação em Geologia (Área
de concentração em Prospecção e Geologia
Econômica), Instituto de Geociências da
Universidade de Brasília, como requisito para
obtenção do título de Mestre em Geologia.

Área de concentração: Geologia Econômica e Prospecção

Orientadora: Prof. Dra. Catarina Laboure Bemfica Toledo

Banca examinadora:

Profa. Dra. Catarina Laboure Bemfica Toledo (orientadora)

Prof. Dr. Álvaro Penteado Crosta, Unicamp (Titular Externo)

Profa. Dr. Susanne Tainá Ramalho Maciel (Membro Interno)

Prof. Dr. Claudinei Gouveia de Oliveira (Suplente Interno)

Brasília

2024

AA447a Almeida, Beatriz
APLICAÇÃO DE TÉCNICAS DE ANÁLISE ESTATÍSTICA MULTIVARIADA
E MACHINE LEARNING PARA O MAPEAMENTO DO FOOTPRINT GEOQUÍMICO
DA MINERALIZAÇÃO DE OURO NO DISTRITO MINEIRO DE JACOBINA /
Beatriz Almeida; orientador Catarina Toledo; co-orientador
Adalene Silva. -- Brasília, 2024.
69 p.

Dissertação (Mestrado em Geologia) -- Universidade de
Brasília, 2024.

1. Análise do componente principal. 2. Self-organizing
maps. 3. Prospecção geoquímica. I. Toledo, Catarina, orient.
II. Silva, Adalene, co-orient. III. Título.

“D. Pedro não desejava apenas que o tempo parasse na Bahia, mas que retrocedesse. Afinal, quando el-rei desautorizou as buscas, havia cerca de 2.000 pessoas (incluindo um frade) catando ouro no rio Itapicuru-mirim, em Jacobina, norte do atual estado da Bahia. A vontade real poderia até frear a mineração baiana, mas nunca paralisá-la.

Mesmo proibida, a busca do ouro em Jacobina nunca cessou.”

-Boa Ventura! A corrida do ouro no Brasil (1697-1810), p.141

AGRADECIMENTOS

Inicio meus agradecimentos pela pessoa que possibilitou e me deu todas as condições para que eu chegasse aonde estou hoje, minha mãe, Raquel. Mãe, obrigada por toda sua dedicação e esforço ao longo de tantos anos para que eu tivesse as melhores condições para conquistar meus sonhos. Obrigada por mesmo agora fora de casa, ser sempre o lugar para onde eu quero voltar.

As minhas orientadoras Catarina e Adalene, obrigada por serem presentes, pelas visitas em Jacobina, pela disponibilidade e pelo acolhimento. A conclusão desse trabalho deve-se muito à motivação, confiança e apoio que vocês me deram ao longo desses anos.

Ao Gab, por ter sido meu maior parceiro durante essa jornada e na vida. Ter sua companhia nesses anos de muito trabalho deixou tudo mais fácil, você foi quem mais me motivou quando eu achei que não conseguiria. Começamos o mestrado juntos, vamos concluir juntos e espero que essa parceria tenha uma vida longa.

Aos grandes amigos que a geologia me deu e que se fazem presentes mesmo com a distância: Gabriel, Luiz, Ana Laura, Brunno e Paula.

Ao geólogo Gustavo Rodovalho, mestrando na USP, agradeço a colaboração nessa pesquisa numa etapa fundamental que gerou resultados brilhantes com o SOM. Juntamente ao Prof. Dr. Cleyton Carneiro idealizador da biblioteca de mapas auto-organizáveis IntraSOM.

A Pan American Silver Corp. agradeço o financiamento, viabilização e fornecimento dos dados para essa pesquisa.

Ao time de exploração da JMC, geólogos, técnicos e auxiliares agradeço pelas trocas diárias, apoio na coleta de dados e suporte para a realização deste trabalho. Agradeço especialmente o apoio durante os últimos três anos dos amigos Matheus, Artur, Daniel, Gabriel Ito, Rodolfo, Claudio, Wesley e Robson.

Ao geólogo Juliano Souza, que foi quem apoiou desde o início a realização dessa pesquisa e permitiu a realização do trabalho.

Finalizo agradecendo à Universidade de Brasília e ao Instituto de Geociências por toda minha formação. A UnB é uma universidade transformadora, aonde fui muito feliz, fiz grandes amigos e vivi experiências inesquecíveis.

O presente trabalho foi realizado com apoio da Coordenação de Aperfeiçoamento de Pessoal de Nível Superior-Brasil (CAPES) – Código de Financiamento 001.

RESUMO

Esta dissertação apresenta os resultados da caracterização do *footprint* geoquímico da mineralização de ouro nos metaconglomerados superiores do Complexo Mineiro de Jacobina, localizado na cidade de Jacobina, Bahia. Os resultados foram alcançados a partir da aplicação de metodologias de análise estatística multivariada e classificação não supervisionada. Para tanto, foram selecionados três corpos mineralizados, João Belo Sul, Canavieiras e Serra do Córrego, que se estendem em direção NS ao longo de 14km na bacia de Jacobina. Um total de 3048 amostras foram coletadas em furos de sondagem realizados nesses três alvos. O processo de amostragem foi feito ao longo de todos os furos com coleta de amostras de 50cm para análises litogeoquímicas. Foram realizadas dosagens de elementos maiores, menores e traço utilizando ICP-MS (Espectrômetro de massa com plasma indutivamente acoplado). Também foram coletadas amostras para confecção de lâminas petrográficas com o objetivo de caracterizar a mineralogia e textura das zonas mineralizadas. Os dados litogeoquímicos foram processados seguindo abordagem para tratamento de dados composicionais e em seguida foram aplicadas metodologias de análise estatística e classificação não supervisionada. A abordagem iniciou-se com estatística univariada a partir de diagramas *boxplot*, seguindo para estatística multivariada com a análise do componente principal (PCA) e finalizando com uma comparação com o algoritmo de mapas auto-organizáveis (SOM). A partir da primeira etapa da análise do componente principal foi possível caracterizar o background geoquímico dos metaconglomerados em cada um dos alvos. Para João Belo Sul obteve-se a associação U-As-Te-Bi-Sb-Pb-Cr-Th-Sr-Hf-Zr-P, ressaltando a afinidade com elementos litófilos e com fases sulfetadas. Na Mina Serra do Córrego a associação Al-Na-Ti-Rb-K-Nb-Sc, tipicamente constituída de elementos litófilos incluindo álcalis, sugere a influência de fluidos hidrotermais na concentração do ouro e, para a Mina Canavieiras, a associação Ni-Fe-Mo-Li-Mg-Mn-Au-S-Co-Cu reflete correlações entre os corpos intrusivos máficos e a mineralização de Au. Em um segundo momento a análise do componente principal foi aplicada novamente com o objetivo de caracterizar a assinatura da mineralização de ouro em cada alvo. Foram identificadas associações entre o ouro e elementos calcófilos. A última etapa foi o emprego de mapas auto-organizáveis para melhor visualização e clusterização das associações geoquímicas. O resultado alcançado pelo SOM se mostrou mais avançado que o resultado da PCA. Além das associações do Au com elementos calcófilos como Ag, As, Sb, Bi, Mo, Pb e Fe, o SOM mapeou outras duas assinaturas para a Mina Canavieiras, Au-Mg-Ni-Zn, interpretado como associado as rochas máficas abundantes neste alvo, e o ouro livre, possivelmente relacionado a mineralização presente em fraturas e falhas geradas durante os eventos tectônicos que afetaram a região. Interpreta-se que a coexistência de três fases de mineralização distintas em Canavieiras é o motivo pelo qual esse alvo apresenta os maiores teores de ouro na área de estudo, ilustrando a importância de fluidos hidrotermais para a reconcentração da mineralização, gerando zonas de alto teor. Os resultados obtidos com essa pesquisa são inovadores e contribuem positivamente com a manutenção dos programas exploratórios na região.

PALVRAS CHAVE: Distrito Mineiro de Jacobina; Análise do componente principal; *Self-organizing maps*; Prospecção geoquímica;

ABSTRACT

This dissertation presents the results of characterizing the geochemical footprint of gold mineralization in the upper metaconglomerates of the Jacobina mining complex, located in the city of Jacobina, Bahia. The outcomes were achieved through the application of statistical analysis and unsupervised classification methodologies. Three mineralized bodies—João Belo Sul, Canavieiras, and Serra do Córrego—were selected, extending in a NS direction for 14 km in the Jacobina basin. A total of 3048 samples were collected from boreholes drilled in these three targets, with a sampling process spanning the entire length of the drillholes and collecting 50cm samples for lithochemical analyses. Multi-element analyses were conducted using ICP-MS (Inductively Coupled Plasma Mass Spectrometry). Additionally, samples were collected for the preparation of petrographic thin sections to characterize the mineralogy and texture of the mineralized zones. The lithochemical data underwent processing following recommendations for compositional data treatment, and subsequently, statistical analysis and unsupervised classification methodologies were applied. The approach began with univariate statistics using boxplot diagrams, followed by multivariate statistics with Principal Component Analysis (PCA), and concluded with a comparison using Self-Organizing Maps (SOM) algorithm. From the initial stage of the Principal Component Analysis, it was possible to characterize the geochemical background of the metaconglomerates in each target. For João Belo Sul, an association of U-As-Te-Bi-Sb-Pb-Cr-Th-Sr-Hf-Zr-P was obtained, emphasizing the affinity with lithophile elements and sulfide phases. In Serra do Córrego, the Al-Na-Ti-Rb-K-Nb-Sc association, typically constituted of lithophile elements including alkalis, suggests the influence of hydrothermal fluids, while for Canavieiras, Ni-Fe-Mo-Li-Mg-Mn-Au-S-Co-Cu reflects correlations between mafic intrusive bodies and Au mineralization. In a subsequent step, Principal Component Analysis was applied again to characterize the gold mineralization signature in each target, identifying associations between gold and chalcophile elements. The final stage involved the use of Self-Organizing Maps for enhanced visualization and clustering of geochemical associations. The SOM results demonstrated a more advanced outcome compared to PCA. Besides associations of Au with chalcophile elements such as Ag, As, Sb, Bi, Mo, Pb, and Fe, SOM mapped two additional signatures for the Canavieiras target: Au-Mg-Ni-Zn, interpreted as associated with the abundant mafic rocks in this target, and free gold, possibly related to mineralization present in fractures and faults generated during tectonic events affecting the Jacobina Basin. It is interpreted that the coexistence of three distinct mineralization phases in Canavieiras is the reason why this target exhibits the highest gold grades in the study area, illustrating the importance of hydrothermal fluids in reconcentrating mineralization, generating high-grade zones. The results obtained from this research are innovative and positively contribute to maintaining exploratory programs in the region.

KEYWORDS: Jacobina Mining District; Principal Component Analysis; Self-Organizing Maps; Geochemical prospecting.

LISTA DE FIGURAS

- Fig. 1.1** - Mapa simplificado de localização da cidade de Jacobina-BA. Em vermelho destaca-se a unidade da Jacobina Mineração a sul do município.....14
- Fig. 1.2** Fluxograma das etapas de trabalho envolvidas nessa pesquisa.....15
- Fig. 2.1.** A) Sketch map of the main geotectonic units of the São Francisco Craton in the Bahia State, Brazil, indicating the area of exposure of the Jacobina Basin rocks (after Teles et al., 2020). B) Simplified geological map of the Jacobina Mountain Range and its surroundings, indicating the location of Jacobina Mine Complex (modified after Santos et al., 2019; Reis et al., 2021; Ferreira et al., 2022)27
- Fig. 2.2.** A) Geological map of the Jacobina Mine Complex with the location of the studied targets – João Belo Sul, Canavieiras and Serra do Córrego – and the identification of cross sections A and B. B) Cross section of Serra do Córrego Formation in the Canavieiras and Serra do Córrego target. C) Cross section of Serra do Córrego Formation in the João Belo Sul target. On B and C the main units that comprise the upper metaconglomerate are identified (Maneira reef, Holandês reef, LVLPC reef, LMPC, reef, MPC reef, SPC reef, MU reef and LU reef).....29
- Fig. 2.3** Stratigraphic column of the Serra do Córrego Formation, Jacobina Group, for the João Belo Sul and Canavieiras/Serra do Córrego targets. In this column, the subunits (reefs) are color-coded based on whether the metaconglomerates are mineralized or barren. Modified after Teles et al. (2015).....31
- Fig. 2.4.** Mineralized metaconglomerate samples and photomicrographs: a) Metaconglomerate sample from LVL reef in Canavieiras mine, well-packed metaconglomerate with quartz and chert pebbles and matrix with intense fuschite-pyrite alteration. b) Drill core sample from LU reef from Serra do Córrego, well-packed metaconglomerate, with intense Fe-oxide alteration and visible gold hosted in fracture. c) and d) Oligomitic (clasts of quartz and chert) metaconglomerate photomicrograph (transmitted polarized light). e) subhedral epigenetic pyrite (Pyrite2) grains associated with fuchsite and rutile marking the foliation. f) Anedral sedimentary pyrite (Pyrite1) strongly altered to Fe-oxide with fuchsite associated and zircon. g) Rounded gold particle in metaconglomerate matrix with anedral pyrite grains. h) Gold included in pyrite pseudomorph. All photomicrographs are of samples from João Belo Sul, except “e”, which is from Canavieiras.38
- Fig. 2.5.** Metaconglomerate samples with visible gold from Jacobina Gold District. A) Gold particles distributed along fracture in sample from LU reef – Canavieiras target; B) Visible gold around quartz pebbles in metaconglomerate sample from MU reef – Canavieiras target; C) Fracture plane with visible gold particles in sample from Main Reef; D) Large dendritic gold particle intercepted in a sample from a drillhole in the Footwall zone.....39
- Fig. 2.6.** Box and whisker plots of selected elements (Au, Ag, As, Bi, Cr, Cu, Fe, Mg, Ni, S, Sc, Th, U and Zr). The circles beyond the limit of the whiskers are outlier samples. Diagrams for the other elements in the dataset can be accessed in the appendix.....41
- Fig. 2.7.** Principal component analysis (PCA) biplot of the first two principal components. PC1 represents 22.7% of the variance and PC2 represents 17.2%. Metaconglomerate samples are colored according to the target.43
- Fig. 2.8.** Results of PCA plotted in a biplot with metaconglomerate samples colored according to the ore content. PCs were selected aiming to better display the mineralized clusters. (A) João Belo Sul PC1 vs. PC2 – mineralized samples are concentrated around the eigenvectors of Mo, Sr, Ag, Pb, Te, Sb, Au, Th, Fe, As and Bi; (B) Canavieiras plot of PC1 vs. PC3 – the samples are grouped into two areas of the diagram. The first marks the association with Au, Cr, Fe, Pb, U, Ag, Mo, Te and Bi. The second group marks the association with Mg, Ni, Zn, Ga, Ti and Sc. (C) Serra do Córrego plot of PC1 vs. PC2 – mineralized samples group around the eigenvectors of As, Au, Te, Pb, U, Sr, Sb, Th, and Bi.47
- Fig. 2.9.** Unified distance matrix (U-matrix) for each of the three datasets. Each neuron is colored representing the distance between the adjacent neurons. Warmer colors represent longer distances, mining more dissimilarity.48
- Fig. 2.10.** Component planes of geochemical variables analyzed in self-organizing map (SOM) presented for each target - (A) Canavieira, (B) João Belo Sul and (C) Serra do Córrego.....49.

Fig. 2.11. Delineation of geochemical associations mapped in SOM for each of the targets. The elemental assemblages correlated to gold mineralization are described in table 2.6.51

LISTA DE TABELAS

Table. 2.1 Abbreviated names and their corresponding meanings for reefs within the Upper Metaconglomerate Unit.....31

Table. 2.2 Macroscopic description of the mineralized zone in the upper metaconglomerate at João Belo Sul target. The first column showcases photographs depicting typical samples from the corresponding reef, sourced from various drillholes. The second column provides a summarized description of each sub-unit.....36

Table. 2.3 Macroscopic description of the mineralized zone in the upper metaconglomerate at Canavieiras and Serra do Córrego targets. The first column features photographs depicting typical samples from the corresponding reef, all obtained from drillholes in Canavieiras. Samples of LVLPC, MU, and LU reefs are derived from the same drillhole. The second column provides a concise summary of each sub-unit.....37

Table. 2.4 Correlation matrix of selected elements from the João Belo Sul dataset. The correlation matrices for Canavieiras and Serra do Córrego can be found in Appendix Table A2.....42

Table 2.5. Table of selected principal components representing the biggest data variability for each target, calculated from transformed geochemical data ($n_{\text{João Belo Sul}} = 1110$ samples; $n_{\text{Canavieiras}} = 1001$ samples; $n_{\text{Serra do Córrego}} = 936$ samples).....44

Table 2.6. Table of the scaled eigenvectors for the most representative PCs, each PC has been sorted individually so all the positive and negative correlations are displayed in order.....46

Table. 2.7. Summarized geochemical signature of gold mineralization identified by principal component analysis and self-organizing maps.....53

Sumário

Capítulo 1	11
1. Introdução	11
1.1 Apresentação	11
1.2 Objetivos.....	13
1.3 Localização.....	15
1.4 Materiais e Métodos	16
1.5 Estrutura da dissertação	20
2. Referências Bibliográficas.....	20
Capítulo 2	25
1. Introduction	26
2. Geological Setting	27
2.1 Regional Geology.....	27
2.2 Jacobina Group.....	29
2.3 Gold Mineralization.....	33
3. Material and Methods.....	34
3.1 Sampling and Geochemical Data	34
3.2 Statistical analysis	34
3.3 Unsupervised machine learning.....	36
4. Results	37
4.1 Field aspects and petrography of Serra do Córrego Formation Upper Metaconglomerate	37
4.2 Whole rock geochemistry.....	42
4.3 Geochemical pattern in PCA space	44
4.4 SOM clustering.....	47
5. Discussion.....	54
5.1 Local geochemical background	54
5.2 Unsupervised learning and the delineation of pathfinder element assemblages	55

6. Conclusion.....	58
Acknowledgments	59
7. References	60
Capítulo 3	65
1. Considerações finais	65
2. Referências bibliográficas	67

Capítulo 1

1. Introdução

1.1 Apresentação

A história da mineração de ouro em Jacobina, Bahia, teve início no século XVIII por volta de 1700 com a chegada dos bandeirantes (Figueiredo, 2012). Em 1722 foi fundada a vila de Jacobina, que alguns anos depois seria elevada à categoria de cidade. Desde sua fundação até os dias atuais, a economia dessa região tem sido fortemente impulsionada pelo setor da mineração, tanto pelo garimpo quanto pela produção industrial.

O complexo mineiro de Jacobina opera desde 1950 por meio de capital externo e grandes empresas já passaram por lá como Anglo American, Desert Sun Mining, Yamana Gold. Desde 2023, as operações estão em posse da Pan American Silver Corp. O complexo conta com cinco minas em operação e possui uma reserva de 3Moz de ouro com um teor médio de 2.02 g/t (Pan American Silver, 2023).

Os depósitos de Jacobina estão alojados na bacia homônima que se estende por cerca de 500km ao longo de um *trend* N-S. Essa bacia de idade arqueana está inserida no contexto do Cráton São Francisco e tem como embasamento gnaisses de composições tonalíticas, trondhjemiticas e granodioríticas (TTG) do Bloco Gavião (Marinho, 1991; Martin et al., 1991; Santos Pinto, 1996; Cunha et al., 1996). A orogenia transamazônica que atuou durante o Paleoproterozoico e resultou na estabilização do cráton, foi responsável pela estruturação da Serra de Jacobina ao longo do lineamento Contendas-Jacobina (Sabaté et al., 1990; Barbosa e Sabaté, 2002, 2004). Essa serra se estende por mais de 200km e é sustentada pelos sedimentos do Grupo Jacobina (Ledru et al. 1997; Milesi et al. 2002; Barbosa and Sabaté 2004; Leite et al. 2007).

A mineralização de ouro ocorre principalmente associada aos metaconglomerados da Formação Serra do Córrego, unidade basal do Grupo Jacobina (Gross, 1968; Pearson et al., 2005; Teles et al., 2015; Reis et al, 2021). Esse forte controle sedimentar da mineralização, caracterizado por corpos tabulares mineralizados com pirita associada e de idades arqueanas a paleoproterozóicas, faz com que os depósitos de Jacobina sejam frequentemente assemelhados aos depósitos de Witwatersrand, África do Sul, e outros depósitos tipo *placer*.

Devido a essa forte associação com a bacia Witwatersrand, a indústria mineira também adotou a nomenclatura de *reefs* para identificar os níveis de metaconglomerado.

São reconhecidas duas unidades principais de metaconglomerado na Formação Serra do Córrego, os inferiores e o superiores que são separados por um espesso pacote de quartzito. Cada uma dessas unidades é individualizada em uma série de *reefs*, alguns mineralizados e outros não.

Além da mineralização hospedada nos metaconglomerados, que está mais associada à matriz da rocha, existe a mineralização fortemente controlada por estruturas, como falhas, fraturas, veios e brechas. Também é comum a mineralização associada aos corpos máficos-ultramáficos que ocorrem ao longo de toda a Formação Serra do Córrego, nesse caso, o ouro pode ocorrer tanto no contato entre os diques e o metaconglomerado, quanto na própria rocha máfica-ultramáfica sendo incluso em piritas ou livre.

Existe muito debate quanto à origem do ouro em Jacobina. Desde o início a discussão foi bastante dividida entre um modelo de mineralização singenética tipo *paleoplacer* (Bateman, 1958) e o modelo hidrotermal epigenético (White, 1956; Davidson, 1957). À medida que novas ideias foram surgindo para o modelo metalogenético da mineralização aurífera hospedada em reefs da Bacia Witwatersrand, essas mesmas ideias foram sendo trazidas para o contexto de Jacobina. Houve então, de um lado, uma evolução do modelo do paleoplacer clássico para o paleoplacer modificado, no qual a ação de fluidos pós-deposicionais na remobilização do ouro é considerada (Gross, 1968; Robb and Meyer, 1991; Frimmel et al., 1993, 2019; Teles et al., 2015, 2020; Garayp and Frimmel, 2023). De outro lado, continuaram surgindo propostas que encaixam os depósitos de Jacobina em um sistema hidrotermal epigenético (Barnicoat et al. 1997; Milesi et al. 2002; Pearson et al., 2005).

Os trabalhos anteriores realizados em Jacobina foram dedicados à investigação da gênese do depósito, com foco nos modelos de mineralização existentes para esse tipo de depósito, incluindo paleoplacer, paleoplacer modificado ou hidrotermal (e.g.: Teixeira et al., 2001; Milési et al, 2002; Pearson et al., 2005). Dentro da abordagem prospectiva de sistemas minerais, essa é uma etapa crucial para programas exploratórios num cenário *greenfield*, o qual requer a definição um modelo geológico preditivo para o tipo de depósito (Groves et al., 2020). Entretanto, para um cenário avançado de prospecção mineral, a pergunta a ser respondida é “quais seriam os principais vetores exploratórios para identificação de novas minas?”. Num contexto como o de Jacobina, onde existe um histórico de mineração em escala industrial há mais de 50 anos, responder essa pergunta é fundamental para maior sucesso dos programas exploratórios. Apesar da resposta ser

muito complexa, o caminho para ela é identificar onde estão as zonas de alto teores hoje, quais os fatores que concentraram a mineralização e quais são os vetores exploratórios que podem otimizar a descoberta de novos alvos mineralizados no Complexo Mineiro Jacobina.

Um caminho para ampliar o entendimento é a utilização de algoritmos de inteligência artificial para modelagem de dados. Dentre vários, o uso de *machine learning* na prospecção mineral é um tópico bastante atual e que tem sido empregado em diversas localidades com o objetivo de extrair maior informação geológica de bancos de dados complexos (Grunsky, 2010; Grunsky e de Caritat, 2020). Esses algoritmos se dividem em aprendizagem supervisionada e não supervisionada. Algoritmos supervisionados são treinados com base em dados já rotulados. Alguns exemplos bastante utilizados nas geociências são: *random forest*, *decision tree* e *k-nearest neighbor* (Breiman et al., 1984, Brown et al., 2000, Abedi et al., 2012, Rodriguez-Galiano et al., 2015). Algoritmos não supervisionados utilizam dados não rotulados para identificar padrões e gerar agrupamentos, como no caso da análise do componente principal (PCA) (Reimann et al. 2008; Hood et al., 2019;) e mapas auto-organizáveis (SOM) (Grunsky, 2010; Grunsky e de Caritat, 2020; Chen et al., 2023).

Neste trabalho foram aplicadas metodologias de classificação não supervisionada a partir de um banco de dados de análises de litogeoquímica com 3048 amostras de metaconglomerado, provenientes dos alvos João Belo Sul, Serra do Córrego e Canavieiras. O objeto de estudo são os metaconglomerados da unidade superior. Esta unidade tem a maior contribuição na produção de ouro do distrito de Jacobina, tanto na massa, quanto no teor médio.

A proposta central desta pesquisa é delinear as assinaturas geoquímicas da mineralização de ouro no Complexo Mineiro de Jacobina, utilizando estatística multivariada através da análise dos componentes principais e mapas auto-organizáveis, a fim de apoiar a continuidade dos trabalhos exploratórios no contexto *near mine*. Neste cenário, a aplicação de metodologias de classificação não supervisionada é uma excelente ferramenta para explorar a estrutura intrínseca do dado e para a identificação de anomalias.

1.2 Objetivos

O objetivo central dessa pesquisa é caracterizar o *footprint* geoquímico da mineralização de ouro no distrito mineiro de Jacobina, utilizando análise dos

componentes principais e mapas auto-organizáveis em dados litogeoquímicos de amostras de furos de sondagem.

Os objetivos específicos compreendem:

- Análise geoquímica univariada, bivariada e multivariada sistemática das amostras do banco de dados de furos de sondagem dos níveis de metaconglomerado mineralizados e estéreis de três alvos: João Belo Sul, Serra do Córrego e Canavieiras;
- Análise de componentes principais para comparação dos dados geoquímicos entre os três alvos e para caracterização do *footprint* geoquímico da mineralização comparando amostras estéreis e mineralizadas.
- Aplicação de mapas auto-organizáveis para caracterizar o *footprint* geoquímico da mineralização nos três alvos;
- Comparar e avaliar a eficácia dos métodos de análise multivariada e rede neural para definição de *footprint* geoquímico da mineralização;
- Delinear os vetores exploratórios para os três alvos estudados visando contribuir para o entendimento do sistema mineral.

1.3 Localização

A área de estudo está localizada na região nordeste do Brasil, município de Jacobina, porção norte do estado da Bahia. O município fica à 330km da capital, Salvador, com acesso pela rodovia BR-324. O complexo mineiro de Jacobina, pertencente a Jacobina Mineração, subsidiária da Pan American Silver Corp., fica na porção sul do município, a 10km da região central (Fig. 1.1).

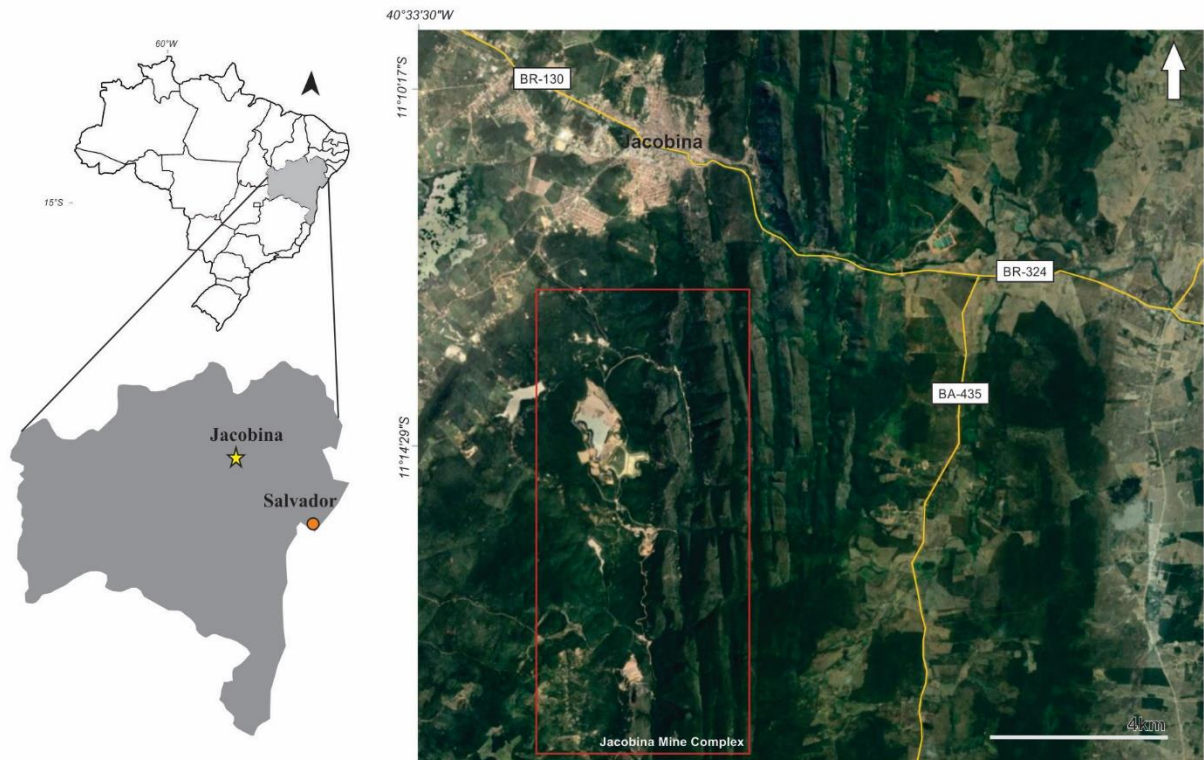


Fig. 1.1 Mapa simplificado de localização da cidade de Jacobina-BA. Em vermelho destaca-se a unidade da Jacobina Mineração a sul do município.

1.4 Materiais e Métodos

O fluxograma abaixo ilustra de forma resumida todas as etapas envolvidas nesta pesquisa (Figura 1.2). Em seguida, uma descrição detalhada de cada uma dessas etapas e das metodologias utilizadas é apresentada.

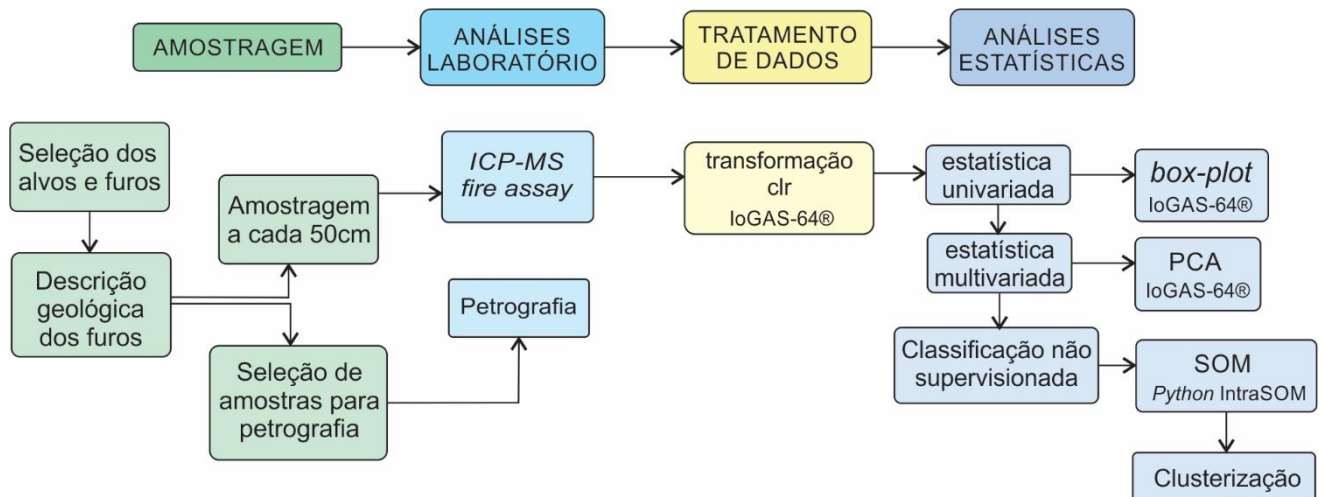


Fig. 1.2 Fluxograma das etapas de trabalho envolvidas nessa pesquisa.

1.4.1 Dados Cartográficos

As bases cartográficas utilizadas nesta pesquisa foram elaboradas pela equipe de exploração da Pan American Silver Corp. – Jacobina Mineração e Comércio (JMC). O mapa geológico (Fig. 4.2) segue a escala 1:5000 e nele estão individualizadas de forma simplificada as grandes unidades da área de estudo – embasamento, metaconglomerado inferior, quartzitos, metaconglomerado superior, Formação Rio do Ouro e diques máficos-ultramáficos. As seções transversais ilustram de forma detalhada a ocorrência da unidade metaconglomerado superior com seus respectivos reefs individualizados. Tanto o mapa quanto as seções foram confeccionados utilizando os softwares ArcGIS Pro e Leapfrog Geo.

1.4.2 Amostragem e análise litogeoquímica

O processo de amostragem para essa pesquisa iniciou-se com a seleção dos alvos a serem estudados, diversos corpos, compõem o Complexo Mineiro de Jacobina. Os três alvos selecionados, João Belo Sul, Serra do Córrego e Canavieiras, oferecem grande potencial de expansão exploratória. Além disso, são alvos que, no momento, estavam com campanhas de sondagem em andamento, o que favoreceu os processos de amostragem e análises laboratoriais.

As amostras utilizadas são provenientes de furos de sondagem que foram executados ao longo dos anos de 2021 e 2022. O terreno bastante acidentado de Jacobina não permite que os furos de sondagem sejam executados seguindo uma malha regular. Por isso, a seleção dos furos em cada um dos alvos foi feita visando a maior equidistância possível entre eles e, também, foram selecionados furos que interceptam toda a sequência dos metaconglomerados superiores.

Primeiramente os testemunhos de sondagem foram descritos pela autora e pela equipe de geólogos do setor de exploração. Nessa etapa são identificados os contatos entre os diferentes tipos de rocha e é feita uma caracterização dos níveis de metaconglomerado, descrevendo o tamanho dos seixos, o grau de empacotamento, tipo de seixos, presença de sulfetos e o grau da alteração metamórfica/hidrotermal. A sistemática de amostragem dos furos seguiu os padrões internos da Jacobina Mineração (JMC), no qual os furos são amostrados a cada 50 cm.

Um total de 3048 amostras foram analisadas para a composição química de elementos maiores, menores e traço. As análises multi-elementares foram realizadas por ICP-MS (espectrometria de massa por plasma indutivamente acoplado) a partir da digestão das amostras com quatro ácidos e foram conduzidas pelo laboratório ALS. As análises de ICP-MS retornaram resultados para 48 elementos, sendo eles, Ag, Al, As, Ba, Be, Bi, Ca, Cd, Ce, Co, Cr, Cs, Cu, Fe, Ga, Ge, Hf, In, K, La, Li, Mg, Mn, Mo, Na, Nb, Ni, P, Pb, Rb, Re, S, Sb, Sc, Se, Sn, Sr, Ta, Te, Th, Ti, Tl, U, V, W, Y, Zn, Zr. O ouro foi analisado por fire-assay.

Algumas amostras também foram coletadas para petrografia com o objetivo de caracterizar a assembleia mineral e texturas das zonas mineralizadas do metaconglomerado superior. Foram utilizadas 23 amostras de furos de sondagem do alvo João Belo Sul e 12 amostras do alvo Canavieiras que foram coletadas nas galerias de subsolo. A petrografia foi realizada com auxílio de microscópio petrográfico (Olympus BX51).

1.4.3 Análises estatísticas

Neste trabalho foram aplicadas as recomendações para lidar com dados composicionais propostas por Martín-Fernández et al. (2012), Buccianti and Grunsky (2014), e Gazley et al. (2015). Os autores sugerem que para tratar elementos com baixas concentrações, deve-se aplicar um método de substituição usando 65% do limite de

detecção (LOD). Essa abordagem é apropriada quando menos de 10% das amostras para o elemento de interesse apresentam valores abaixo do LOD. Se mais de 30% das amostras para um dado elemento estiverem abaixo do LOD, esse elemento deve ser descartado. Aqui, os elementos Be, Ca, Cd, Ge, In, Re, Se, Sn, Ta e Tl foram excluídos por mais de 30% das amostras estarem abaixo do limite de detecção.

Dados composicionais são tipicamente expressos como dados "fechados", o que significa que representam partes de um todo e, portanto, exibem correlações intrínsecas entre si. Lidar com dados composicionais brutos pode levar a interpretações equivocadas, principalmente devido à sua tendência a valores positivos e soma igual uma constante. Isso significa que quando um valor muda, os outros também devem mudar para manter a proporção. Para enfrentar esse desafio, técnicas de transformação de razão logarítmica introduzidas por Aitchison (1982) foram adotadas. Essas transformações criam um espaço de amostra com valores positivos e negativos, permitindo a aplicação de estatísticas clássicas e, portanto, uma melhor interpretação das relações e padrões dentro dos dados geoquímicos. Aqui, a transformação da razão logarítmica central (CLR) foi aplicada ao conjunto de dados bruto. A transformação CLR é calculada com base na média geométrica das variáveis dentro de um conjunto de dados. Por esse motivo, é necessário ter um conjunto de dados completo, ou seja, o número de amostras de cada variável deve ser o mesmo. O pré-processamento dos dados geoquímicos e a transformação CLR foram realizados usando o software IMDEX ioGas-64 da Reflex.

O trabalho de Filzmoser et al. (2009b) discute sobre a questão do uso de dados composicionais não transformados ou transformados na aplicação de estatística univariada, como *boxplot*. Os autores mostram que uma variável composicional não pode ser tratada separadamente do resto da composição total da amostra. Por isso, mesmo para análises estatísticas mais simples o primeiro passo é “abrir” o banco de dados aplicando uma transformação logarítmica e tornando o dado mais simétrico. Seguindo essa recomendação, o dado transformado foi usado para iniciar a visualização do comportamento das variáveis dentro do sistema mineral de Jacobina a partir de diagramas *boxplot* que são amplamente utilizados na análise exploratória de dados (EAD) (Grunsky et al., 2024).

O fluxograma, GeoCoDa, apresentado por Grunsky et al. (2024) para tratar de dados composicionais litogeoquímicos coloca metodologias de classificação não supervisionada como etapa fundamental para identificação de anomalias geoquímicas.

Algoritmos *machine learning* têm sido amplamente utilizados para essa função, principalmente porque a análise geoquímica gera conjuntos de dados de alta dimensionalidade correlacionados entre si. Essa complexidade representa um desafio significativo na identificação de padrões e na realização de interpretações significativas. Para lidar com isso, métodos não supervisionados como a análise de componentes principais (PCA) e mapas auto-organizáveis (SOM) têm sido efetivamente aplicados para caracterizar padrões geoquímicos associados à mineralização.

A Análise de Componentes Principais (PCA) é uma técnica de classificação não supervisionada amplamente reconhecida que encontra ampla aplicação no tratamento de conjuntos de dados multivariados. Sua principal vantagem está na capacidade de reduzir a dimensionalidade dos dados, mantendo informações essenciais do conjunto de dados original (Jolliffe e Cadima, 2016). A PCA opera criando variáveis artificiais derivadas de uma matriz de correlação. Essas novas variáveis preservam a maior variância presente no conjunto de dados e não são correlacionadas entre si. Essas variáveis recém-geradas, conhecidas como componentes principais (PCs), podem ser visualizadas em um diagrama 2D, alinhando-se ao longo das direções de máxima variância nos dados, onde o primeiro PC é a maior variância, o segundo PC é a segunda maior, e assim por diante. A soma da contribuição percentual de cada PC para a variância dos dados é uma ferramenta fundamental para avaliar a qualidade da redução da dimensionalidade dos dados, embora o foco na PCA esteja quase sempre nos primeiros componentes (Jolliffe e Cadima, 2016). Aqui, a PCA foi usada para produzir grupos geoquímicos no IMDEX ioGas-64 da Reflex.

Comparar diferentes métodos é uma prática valiosa no processo de reconhecimento de padrões geoquímicos (Zuo, 2021). Tendo isso em vista, neste trabalho são empregados mapas auto-organizáveis (SOM) (Kohonen, 1990, 1997), um tipo de rede neural que opera com redução de dimensionalidade e agrupamento de dados. Como outras redes neurais, o SOM trabalha com uma camada de entrada e uma camada de saída. Na camada de saída, os neurônios estão interconectados representando uma região específica do espaço de entrada (Gouvêa et al., 2023). No SOM, cada item de dados é mapeado em um ponto (nódulo) no mapa, e as distâncias dos itens no mapa refletem similaridades entre os itens (Kohonen, 2013). O número de neurônios (M) na camada de saída pode ser determinado usando uma regra heurística (Vesanto and Alhoniemi, 2000), onde N é o número de variáveis de entrada (1).

$$M = 5\sqrt{N} \quad (1)$$

O SOM se mostra uma excelente ferramenta de visualização, fornecendo um diagrama da matriz-U e mapas para cada atributo no conjunto de dados. A matriz-U é um mapa topográfico da rede do SOM, destaca visualmente as regiões da rede onde os dados são mais semelhantes (menores distâncias) e onde são mais diferentes (maiores distâncias). Juntamente com os mapas de componente, que fornece uma visualização intuitiva das relações e disposição espacial do conjunto de dados. Utilizamos o IntraSOM, uma biblioteca em Python desenvolvida pela Escola Politécnica da Universidade de São Paulo, que implementa mapas auto-organizáveis com treinamento em mapas hexagonais toroidais (Gouvêa et al., 2023).

1.5 Estrutura da dissertação

A dissertação de mestrado foi compartimentada em três capítulos. O primeiro capítulo apresenta o histórico da área de estudo, breve contextualização da geologia local e dos métodos empregados. O segundo capítulo compreende o artigo intitulado “Tracing Mineral System Geochemical Footprint with Unsupervised Learning: Jacobina gold district case study” a ser submetido após a defesa. O artigo completo apresenta os resultados da pesquisa, com a descrição da metodologia utilizada, resultados obtidos e discussões com o objetivo de caracterizar as assinaturas geoquímicas dos depósitos de ouro de Jacobina. O terceiro capítulo conclui a dissertação com as considerações finais para a aplicação das metodologias estudadas dentro da rotina de prospecção mineral. A pesquisa foi desenvolvida no Instituto de Geociências da Universidade de Brasília, sob a orientação da Professora Dra. Catarina Labouré Bemfica Toledo e co-orientação da Profa. Adalene Moreira Silva, dentro do Grupo de Pesquisa CNPq - Geodinâmica de Terrenos Pré-Cambrianos e Sistemas Minerai s Associados (SisMineral).

2. Referências Bibliográficas

Abedi, M., Torabi, S. A., Norouzi, G.-H., & Hamzeh, M. (2012). ELECTRE III: A knowledge-driven method for integration of geophysical data with geological and geochemical data in mineral prospectivity mapping. *Journal of Applied Geophysics*, 87, 9–18. <https://doi.org/10.1016/j.jappgeo.2012.08.003>

Aitchison, J. (1982). The Statistical Analysis of Compositional Data. *Journal of the Royal Statistical Society: Series B (Methodological)*, 44(2), 139–160. <https://doi.org/10.1111/j.2517-6161.1982.tb01195.x>

- Barbosa, J. S. F., & Sabaté, P. (2004). Archean and Paleoproterozoic crust of the São Francisco Craton, Bahia, Brazil: geodynamic features. *Precambrian Research*, 133(1–2), 1–27. <https://doi.org/10.1016/j.precamres.2004.03.001>
- Bateman, J. D. (1958). Uranium-bearing auriferous reef at Jacobina, Brazil. *Economic Geology*, 53, 417–425.
- Breiman, L., Friedman, J., Stone, C.J., Olshen, R.A., 1984. Classification and Regression Trees. CRC press.
- Brown, W.M., Gedeon, T., Groves, D., Barnes, R., 2000. Artificial neural networks: a new method for mineral prospectivity mapping. *Aust. J. Earth Sci.* 47, 757–770.
- Buccianti, A. & Grunsky, E. (2014). Compositional data analysis in geochemistry: Are we sure to see what really occurs during natural processes? *Journal of Geochemical Exploration*. 141. 10.1016/j.gexplo.2014.03.022.
- Chen, Z., Xiong, Y., Yin, B., Sun, S., & Zuo, R. (2023). Recognizing geochemical patterns related to mineralization using a self-organizing map. *Applied Geochemistry*, 151, 105621. <https://doi.org/10.1016/j.apgeochem.2023.105621>
- Cunha, J.C. et al. (1996). Idade dos Greenstone belts e dos Terrenos TTGs Associados da Região do Cráton do São Francisco (Bahia, Brasil). In: CONGRESSO BRASILEIRO DE GEOLOGIA, 39., 1996, Salvador. Anais... Salvador: SBG, 1996. v.1, p.62-65.
- Davidson, C.F. (1957). On the occurrence of uranium in ancient conglomerates. *Economic Geology*, 52, p. 668-693.
- Figueiredo, L. (2012). *BOA VENTURA! A CORRIDA DO OURO NO BRASIL (1697-1810)*. (Record, Ed.; 5°).
- Filzmoser, P., Hron, K., Reimann, C., 2009b. Univariate statistical analysis of environmental (compositional) data: problems and possibilities. *Sci. Total Environ.* 407, 6100–6108. <https://doi.org/10.1016/J.SCITOTENV.2009.08.008>.
- Frimmel, H. E., le Roex, A. P., Knight, J., & Minter, W. E. L. (1993). A case study of the postdepositional alteration of the Witwatersrand Basal Reef gold placer. *Economic Geology*, 88(2), 249–265. <https://doi.org/10.2113/gsecongeo.88.2.249>
- Frimmel, Hartwig. (2019). The Witwatersrand Basin and Its Gold Deposits: Methods and Protocols. 10.1007/978-3-319-78652-0_10.
- Gazley, M., Collins, K., Roberston, J., Hines, B., Fisher, L., McFarlane, A., 2015. Application of principal component analysis and cluster analysis to mineral exploration and mine geology. In: AusIMM New Zealand Branch Annual Conference 2015. Australasian Institute of Mining and Metallurgy (AusIMM), New Zealand Branch, Dunedin, pp. 131–139.

Garayp, E., & Frimmel, H. E. (2023). A modified paleoplacer model for the metaconglomerate-hosted gold deposits at Jacobina, Brazil. *Mineralium Deposita*. <https://doi.org/10.1007/s00126-023-01220-9>

Gouvêa, R. C. T., Gioria, R. dos S., Marques, G. R., & Carneiro, C. de C. (2023). IntraSOM: A comprehensive Python library for Self-Organizing Maps with hexagonal toroidal maps training and missing data handling. *Software Impacts*, *17*, 100570. <https://doi.org/10.1016/j.simpa.2023.100570>

Gross, W. H. (1968). Evidence for a Modified Placer Origin for Auriferous Conglomerates, Canavieiras Mine, Jacobina, Brazil. In *Economic Geology* (Vol. 63).

Groves, D. I., Santosh, M., & Zhang, L. (2020). A scale-integrated exploration model for orogenic gold deposits based on a mineral system approach. *Geoscience Frontiers*, *11*(3), 719–738. <https://doi.org/10.1016/j.gsf.2019.12.007>

Grunsky, E.C., (2010). The interpretation of geochemical survey data. *Geochem. Explor. Environ. Anal.* *10*, 27–74.

Grunsky, E., de Caritat, P., (2020). State-of-the-art analysis of geochemical data for mineral exploration. *Geochem. Explor. Environ. Anal.* *20*, 217–232.

Grunsky E., Greenacre M., Kjarsgaard, B. (2024). GeoCoDA: Recognizing and validating structural processes in geochemical data. A workflow on compositional data analysis in litho geochemistry. *Applied Computing and Geosciences*.100149. ISSN 2590-1974. <https://doi.org/10.1016/j.acags.2023.100149>

Hood, S. B., Cracknell, M. J., Gazley, M. F., & Reading, A. M. (2019). Element mobility and spatial zonation associated with the Archean Hamlet orogenic Au deposit, Western Australia: Implications for fluid pathways in shear zones. *Chemical Geology*, *514*, 10–26. <https://doi.org/10.1016/j.chemgeo.2019.03.022>

Jolliffe, I. T., & Cadima, J. (2016). Principal component analysis: a review and recent developments. *Philosophical Transactions of the Royal Society A: Mathematical, Physical and Engineering Sciences*, *374*(2065), 20150202. <https://doi.org/10.1098/rsta.2015.0202>

Kohonen, T. (1990). The self-organizing map. *Proceedings of the IEEE*, *78*(9), 1464–1480. <https://doi.org/10.1109/5.58325>

Kohonen, T. (1997). *Self-Organizing Maps* (Vol. 30). Springer Berlin Heidelberg. <https://doi.org/10.1007/978-3-642-97966-8>

Kohonen, T. (2013). Essentials of the self-organizing map. *Neural Networks*, *37*, 52–65. <https://doi.org/10.1016/j.neunet.2012.09.018>

Ledru, P., Milési, J. P., Johan, V., Sabate, P., & Maluski, H. (1997). Foreland basins and gold-bearing conglomerates: a new model for the Jacobina Basin (São Francisco province, Brazil). *Precambrian Research*, *86*(3–4), 155–176. [https://doi.org/10.1016/S0301-9268\(97\)00048-X](https://doi.org/10.1016/S0301-9268(97)00048-X)

Leite, C., Barbosa, J., Nicollet, C., & Sabaté, P. (2007). Evolução metamórfica/metassomática Paleoproterozóica do Complexo Saúde, da Bacia de Jacobina e de leucogranitos peraluminosos na parte norte do Cráton do São Francisco. *Revista Brasileira De Geociências*, 37, 777–797.

Marinho, M.M. (1991) La sequence volcano-sedimentaire de Contendas-Mirante et la bordure occidentale du Bloc de Jequié (Craton do São Francisco), Brésil: un exemple de transition archéen-proterozoic. Clermont-Ferrand n, 345p. (Tese - Doutorado) - Université Blaise Pascal.

Martin, H. (1987) Archaean and modern granitoids as indicators of changes in geodynamic processes. *Revista Brasileira de Geociências*, v.17, n.4, p.360-365.

Milesi, J. P., Ledru, P., Marcoux, E., Mougeot, R., Johan, V., Lerouge, C., Sabaté, P., Bailly, L., Respaut, J. P., & Skipwith, P. (2002). The Jacobina Paleoproterozoic gold-bearing conglomerates, Bahia, Brazil: a “hydrothermal shear-reservoir” model. *Ore Geology Reviews*, 95–136. www.elsevier.com/locate/oregeorev

Pan American Silver Corp. Annual Report (2023).

Pearson WN, Macedo P M, Rubio A, Lorenzo C L, Karpeta P (2005). Geology and gold mineralization of the Jacobina Mine and Bahia Gold Belt, Bahia, Brazil, and a comparison to Tarkwa and Witwatersrand. *Window to the World: 2005 Symposium Proceedings Geological Society of Nevada, Reno/Sparks Nevada*, pp 757–785

Reimann, C.; Filzmoser, P.; Garrett R.; Dutter R. (2008) Statistical data analysis explained. Applied environmental statistics with R 1 ed. Chichester. Ed. John Wiley 8 Sons, 362 p.

Reis, C et al. (2021). Projeto Integração Geológica E Avaliação Do Potencial Metalogenético Da Serra De Jacobina E Do Greenstone Belt Mundo Novo. Informe de Recursos Minerais, Série Províncias Minerais do Brasil 31 CPRM pp 169. <https://doi.org/10.1111/j.1365-3121.2007.00764.x>

Robb, L. J., & Mayer, F. M. (1991). A contribution to recent debate concerning epigenetic versus syngenetic mineralization processes in the Witwatersrand basin. *Economic Geology*, 86, 396–401.

Rodriguez-Galiano, V., Sanchez-Castillo, M., Chica-Olmo, M., Chica-Rivas, M., 2015. Machine learning predictive models for mineral prospectivity: an evaluation of neural networks, random forest, regression trees and support vector machines. *Ore Geol. Rev.* 71, 804–818.

Sabaté, P.; Marinho, M.M.; Vidal, P.; Cahen-Vachette, M. (1990). The 2-Ga peraluminous magmatism of the Jacobina-Contendas Mirante belts (Bahia, Brazil): Geologic and isotopic constraints on the sources. *Chemical. Geol.*, 83:325-338.

Santos Pinto, M.A. Le recyclage de la croûte continentale archéenne: Exemple du Bloc Gavião – Bahia-Brésil. (1996). 193 f. Tese (Doutorado) - Université de Rennes, Rennes – França, 1996. (Memoires de Geosciences Rennes, 75).

Teles, G., Chemale, F., & de Oliveira, C. G. (2015). Paleoproterozoic record of the detrital pyrite-bearing, Jacobina Au-U deposits, Bahia, Brazil. *Precambrian Research*, 256, 289–313. <https://doi.org/10.1016/j.precamres.2014.11.004>

Teles, G. S., Chemale, F., Ávila, J. N., Ireland, T. R., Dias, A. N. C., Cruz, D. C. F., & Constantino, C. J. L. (2020). Textural and geochemical investigation of pyrite in Jacobina Basin, São Francisco Craton, Brazil: Implications for paleoenvironmental conditions and formation of pre-GOE metaconglomerate-hosted Au-(U) deposits. *Geochimica et Cosmochimica Acta*, 273, 331–353. <https://doi.org/10.1016/j.gca.2020.01.035>

Teixeira, J. B. G., de Souza, J. A. B., da Silva, M. D. G., Leite, C. M. M., Barbosa, J. S. F., Coelho, C. E. S., Abram, M. B., Filho, V. M. C., & Iyer, S. S. S. (2001). Gold mineralization in the Serra de Jacobina region, Bahia Brazil: Tectonic framework and metallogenesis. *Mineralium Deposita*, 36(3–4), 332–344. <https://doi.org/10.1007/s001260100174>

White, M. G. (1956). Uranium in the Serra de Jacobina, State of Bahia, Brazil – Peaceful Uses of Atomic Energy (UNO) – Vol. pág. 140-142

Vesanto, J., & Alhoniemi, E. (2000). Clustering of the self-organizing map. *IEEE Transactions on Neural Networks*, 11(3), 586–600. <https://doi.org/10.1109/72.846731>

Zuo, R., Wang, J., Xiong, Y., & Wang, Z. (2021). The processing methods of geochemical exploration data: past, present, and future. *Applied Geochemistry*, 132, 105072. <https://doi.org/10.1016/j.apgeochem.2021.105072>

*Capítulo 2***Tracing Mineral System Geochemical Footprint with Unsupervised Learning: a case study of the Jacobina gold district**

Beatriz Dantas Rabelo de Almeida^a, Catarina Laboure Bemfica Toledo^a, Adalene Moreira Silva^a, Gustavo Rodovalho Marques^b, Gabriel da Silva Seidler^a

a. Instituto de Geociências, Universidade de Brasília, 70910-900, Brasília, DF, Brazil

b. Instituto de Geociências, Universidade de São Paulo, 05508-080, São Paulo, Brazil

** Corresponding author. E-mail address: beatrizdantas97@gmail.com (B.D.R Almeida).*

ABSTRACT

Unsupervised learning algorithms stand as a powerful contemporary tool for mapping the geochemical footprint of mineral deposits, enhancing the efficiency of exploration programs. Defining indicator associations for mineralization amplifies the efficacy of these programs. In this study, unsupervised learning is employed to identify indicative signatures associated with gold mineralization in three targets – João Belo Sul, Canavieiras e Serra do Córrego – located in the Jacobina mining district, Bahia, Brazil. Principal component analysis is initially utilized to map the background geochemical signatures within the package of upper metaconglomerates, extending along 14 kilometers the NS trend of the basin. Metaconglomerates from each one of the three targets reveal a different geochemical signature: João Belo Sul (U-As- Te-Bi-Sb-Pb-Cr-Th-Sr- Hf-Zr-P), Serra do Córrego (Al- Na-Ti-Rb-K-Nb-Sc) and Canavieiras (Z-Cu-Co-S-Au-Ni-Fe-Mo-Li-Mg-Mn). For the delineation of the geochemical footprint of gold mineralization, in addition to multivariate analysis, neural networks are applied using self-organizing maps. The association of Au with chalcophile elements, such as, Ag, As, Fe, Sb, Bi, Mo and Pb indicates that most of the gold is associated with pyrite. For the Canavieiras target, signatures of free gold and gold correlated with mafic-ultramafic bodies, Au-Mg-Ni-Zn, also stand out. The mapped geochemical patterns favor a dynamic mineral system, where the overlap of different mineralization phases contributed to a higher concentration of gold in Canavieiras target. The SOM results demonstrates a more advanced outcome compared to PCA, allowing the identification of relevant geochemical associations.

Keywords: Unsupervised learning; Geochemical footprint; Principal component analysis; Self-organizing maps; Jacobina gold deposits.

1. Introduction

In the 1970s the concept of “mineral system” emerged in the oil and gas industry. The idea of understanding all geological processes involved in the formation and preservation of a mineral deposit also found its way into mineral exploration a few decades later (McCuaig et al., 2010). This strategy was introduced by Wyborn et al. (1994) in the ore industry, as it became increasingly harder to find new positive prospects. Geologists realized that to achieve success in mineral exploration, it would be necessary to understand the deposit in a larger scale. Since then, investments in new prospective techniques using geochemistry, geophysics and structural geology, have significantly increased. The integration of litho-geochemistry with modern data analysis techniques enriches our understanding of a mineral system, providing valuable insights regardless of the geochemical footprint of an ore deposit and facilitates the delineation of prospective targets (Grunsky and Caritat, 2010; Zuo, 2011; Torppa et al., 2019; Grunsky and Caritat, 2020; Zuo et al., 2021; Sadeghi et al., 2024).

Multivariate analysis techniques have been successfully applied to complex datasets, such as compositional data, to understand the relationships between the variables in the dataset and identify patterns in their interactions. Among these techniques, Principal Component Analysis (PCA) is the most widely used for mapping geochemical anomalies related to mineralization, providing insights into mineralizing processes. Hood et al. (2019) applied PCA to produce groups of elements associated with the protolith and mineralization in the orogenic gold deposit of Hamlet, Western Australia. Grunsky and de Caritat (2020) explored this tool for mapping the potential for metal deposits on the Melville Peninsula, Canada.

Data-driven machine learning methods take a more advanced step in identifying patterns among variables by grouping similar data. Self-organizing maps are an unsupervised methodology based on artificial neural networks that provides dimensionality reduction and clustering. This technique was effectively applied by Torppa et al. (2015) to investigate prospective potential in areas in Finland.

The Jacobina Basin located in Bahia, northeast of Brazil, hosts gold bearing metaconglomerates that have been continuously mined since the 18th century. Due to its clear lithological and sedimentary control over mineralization, there is a strong association of Jacobina gold district to Witwatersrand mineralization and other paleoplacer-like deposits.

This gold district is settled in an Archean terrain that underwent a major amalgamation event during the Paleoproterozoic, the Transamazonian Orogeny. To deepen our understanding of the Jacobina mineral system, it is essential to understand the role of hydrothermal fluids migrating through the basin and define the elemental assemblage linked to gold-bearing metaconglomerates.

To conduct our studies, three targets were selected: João Belo Sul, Serra do Córrego and Canavieiras. Canavieiras has been documented since the 1950s with the highest gold productions and the highest grade within the Jacobina district (Gross, 1968; Milesi et al., 2002; Pearson, 2005). To this day, this mine continues to have the greatest contribution to the annual gold production (Wafforn et al., 2023).

In this paper, we investigated the geochemical footprint of gold-bearing metaconglomerates from Jacobina using unsupervised learning algorithms. To conduct a reliable geochemical pattern recognition process, two different methods are introduced. Firstly, PCA was used to identify the main elements related to gold mineralization. Based on these elements, SOM was applied to create visual interpretation of the relation between the variables.

2. Geological Setting

2.1 Regional Geology

The Jacobina Gold district is situated along a significant NNE-oriented structure that spans an impressive length of over 500 kilometers. This prominent lineament, known as the Contendas-Jacobina, represents the collision zone between three Archean blocks: Gavião, Serrinha and Jequié (Barbosa and Sabaté, 2004) (Fig. 2.1A). This collision event took place during the Paleoproterozoic and played a crucial role in the formation and stabilization of the São Francisco Craton (Almeida, 1977), occurring between 2.1 Ga - 1.91 Ga.

The Jacobina Group is a prominent mountain range stretching over 200 kilometers in a north-south alignment, situated on the eastern margin of the Gavião block (Fig. 2.1B). This group is underlain by Archean rocks from the Gavião block, predominantly composed of TTG (tonalite-trondhjemite-granodiorite) and associated supracrustal rocks. The TTG suite is dated at 3.4 and 3.0 Ga and underwent regionally amphibolite-facies metamorphism during the orogeny. Associated greenstone belt sequences, such as Mundo Novo, are composed of komatiites, tholeiitic basalts, volcanoclastics, and clastic chemical-exhalative rocks ranging in age from 3.2 to 3.4 Ga (Barbosa and Sabaté, 2004).

Younger bodies dated at 2.0 Ga comprise late- to post-tectonic granitic intrusions occurring all along the Contendas-Jacobina Lineament (Sabaté et al., 1990).

The structural framework that controls the entire Jacobina Range was predominantly formed in the Transamazonian orogeny during the Paleoproterozoic. A period when a complex fault system developed in compressional and transpressional phases (Fig. 2.1B). From these, three first-order faults emerge – Pindobaçu, Maravilha, and Jacobina – which bound the entire extent of the basin (Santos et al., 2019).

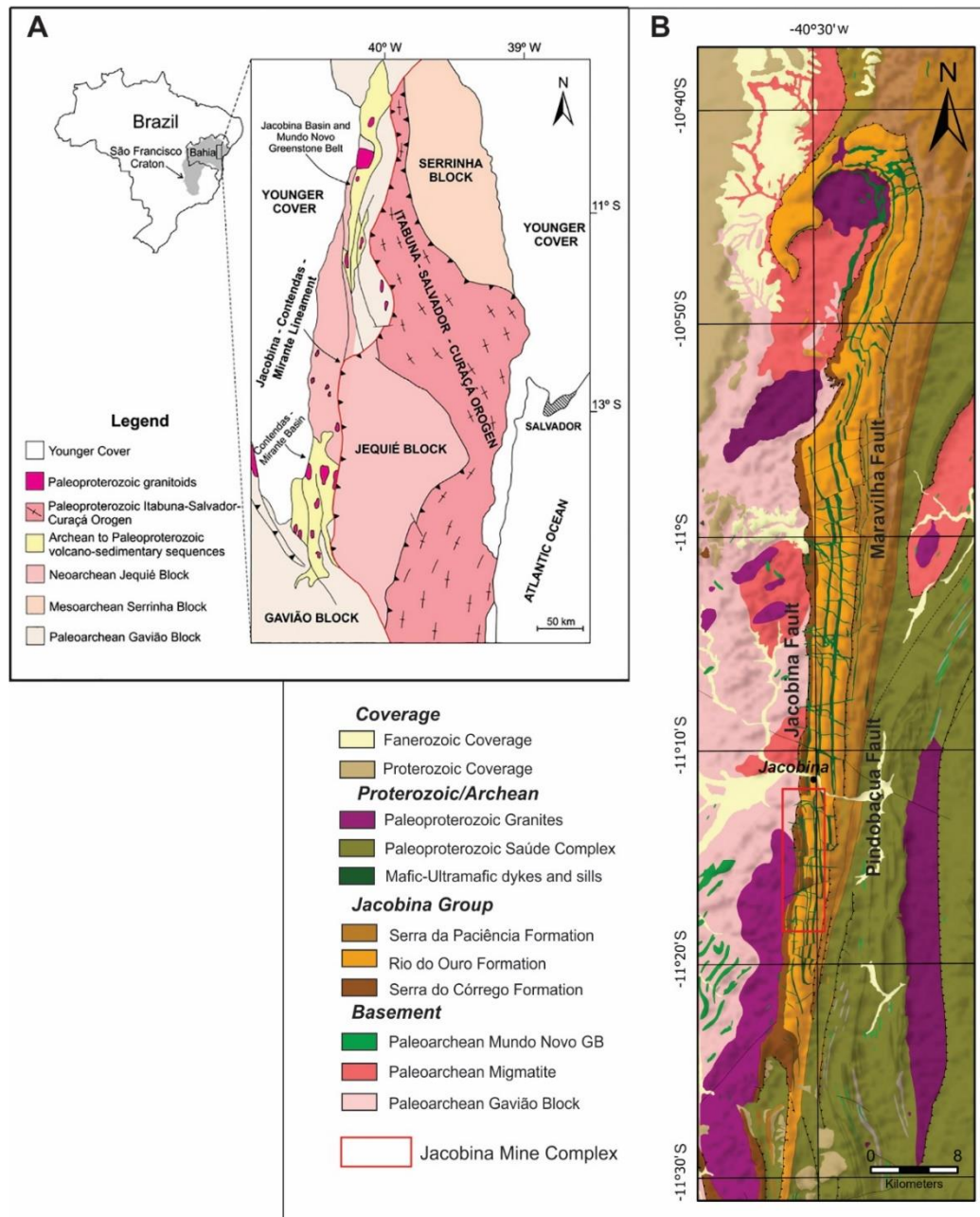


Fig. 2.1. A) Sketch map of the main geotectonic units of the São Francisco Craton in the Bahia State, Brazil, indicating the area of exposure of the Jacobina Basin rocks (after Teles et al., 2020). B) Simplified geological map of the Jacobina Mountain Range and its surroundings, indicating the location of Jacobina Mine Complex (modified after Santos et al., 2019; Reis et al., 2021; Ferreira et al., 2022)

2.2 *Jacobina Group*

Leo et al. (1964) were the first to describe the Jacobina Group. Since then, many stratigraphic models have been proposed considering the tectonic evolution of the basin. The main challenges and controversy when characterizing ancient rocks from the Jacobina Group are related to the lack of well-preserved stratigraphic contacts and the structural complexity of a terrane that underwent a significant amalgamation event.

Although other authors argue that the deposition of the Jacobina Group happened in a foreland basin developed during the Transamazonian Orogeny (2.0 Ga) (Ledru et al., 1997; Milesi et al., 2002; Leite and Marinho, 2012), the most widely accepted model for the tectonic evolution of the basin is the rift model (Mascarenhas et al., 1992; Teles et al., 2015; Santos et al., 2019). In the rift model, the Jacobina Group deposition happened in a pre-GOE (Great Oxidation Event) environment (>2.3 Ga) and the source of the sediments are the Archean rocks of Gavião Block. This model is supported by the description of rounded detrital pyrites and U-Pb ages between 3.3 and 3.4 Ga. (Teixeira et al., 2001; Pearson et al., 2005; Teles et al., 2015; Santos et al., 2019).

The extension of Jacobina Basin is also much debated, with some authors considering the formations Cruz das Almas and Bananeiras as part of the Jacobina Group (Leo, 1964; Leite, 2002; Leite et al., 2007; Reis et al., 2021), while others interpret both formations as part of Mundo Novo greenstone belt (Pearson, 2005; Teles, 2015). The stratigraphic model followed for the Jacobina Group is the one proposed by Pearson (2005) and Teles et al. (2015), which consists of, from the base to the top, Serra do Córrego, Rio do Ouro and Serra da Paciência formations.

The basal unit of the Jacobina Group is the Serra do Córrego Formation, consisting of layered metaconglomerates, quartzites and schists. The deposition of this unit is associated with an alluvial-fluvial system. The metaconglomerates are dominantly oligomictic, with a predominant composition of quartz pebbles. Their color ranges from green to red, which depends on the abundance of the fuchsite alteration or the degree of oxidation (Fig. 2.4a-b).

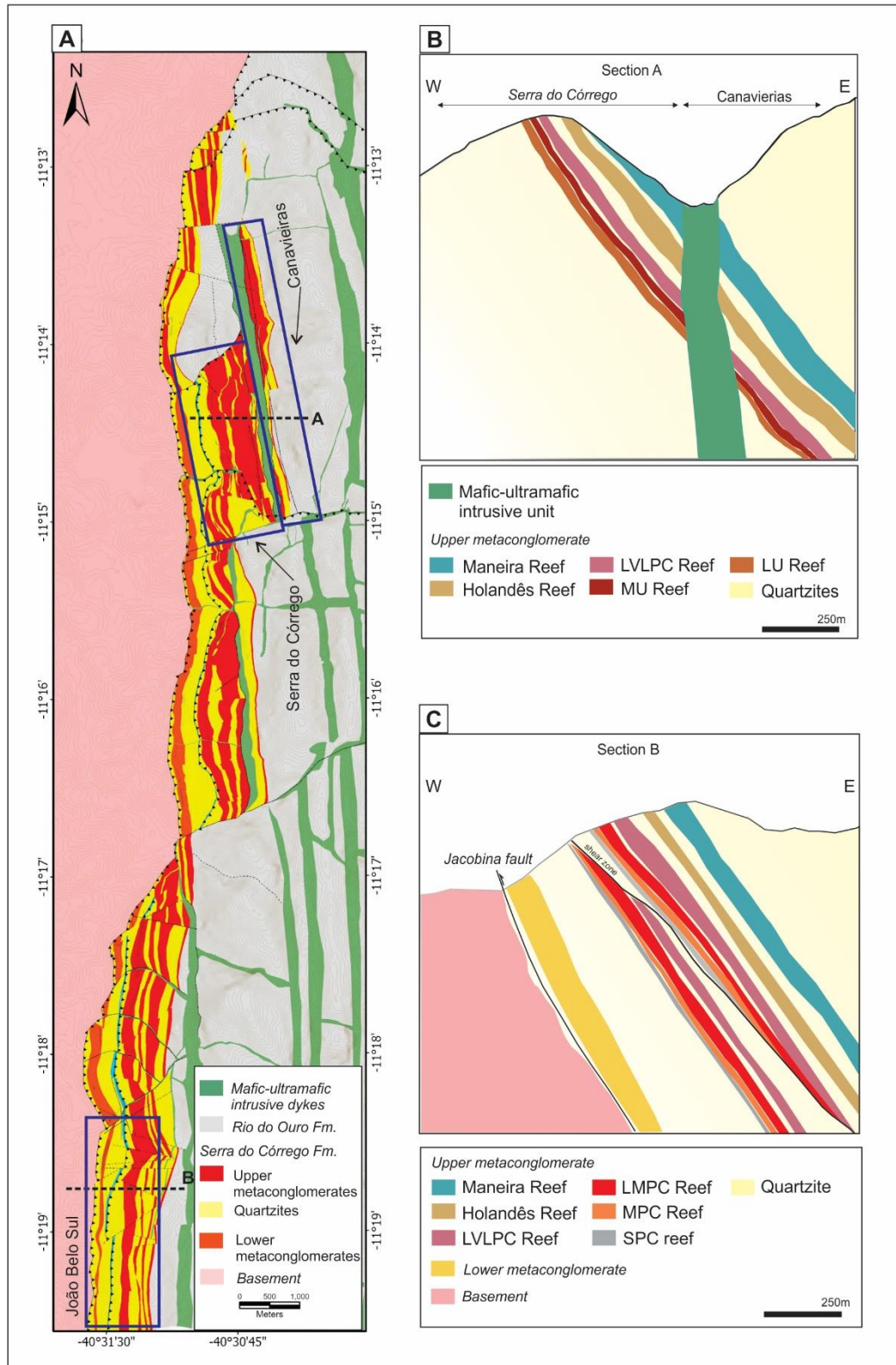


Fig. 2.2. A) Geological map of the Jacobina Mine Complex with the location of the studied targets – João Belo Sul, Canavieiras and Serra do Córrego – and the identification of cross sections A and B. B) Cross section of Serra do Córrego Formation in the Canavieiras and Serra do Córrego target. C) Cross section of Serra do Córrego Formation in the João Belo Sul target. On B and C the main units that comprise the upper metaconglomerate are identified (Maneira reef, Holandês reef, LVLPC reef, LMPC, reef, MPC reef, SPC reef, MU reef and LU reef).

The metaconglomerates from Serra do Córrego formation are individualized into two zones, the Lower Metaconglomerate and the Upper Metaconglomerate (Fig. 2.2 and 2.3). A thick quartzite layer, named Intermediate Quartzite, separates these two main units. Together these three units range in total thickness from 500m to 1,200m. The Lower and Upper Metaconglomerates are also individualized in *reefs* (metaconglomerate beds) (Fig.2.2 B-C). The reefs abbreviated names and their meanings are listed in table 2.1.

Each reef can be characterized not only by the stratigraphical position, but also by the dominant pebble size, that varies from very small (<0.3 mm) to very large (>64 mm). Also, the reefs are separated by quartzite layers that can vary from 4m to 15m thick. The spatial distribution of Serra do Córrego Formation along Jacobina Basin is complex. The basement topographic creates deeper and shallower zones within the basin which directly affects the lateral continuity of the reefs.

Table. 2.1 Abbreviated names and their corresponding meanings for reefs within the Upper Metaconglomerate Unit.

Upper metaconglomerate reefs	
<i>Abbreviation</i>	<i>Meaning</i>
LVLPC	Large - very large pebble metaconglomerate
LMPC	Large - medium pebble metaconglomerate
MU	Medium unit
MPC	Medium pebble metaconglomerate
LU	Lower unit
SPC	Smal pebble metaconglomerate

Rio do Ouro is the central unit of Jacobina basin and it is in a gradational contact with Serra do Córrego formation. This unit comprises a thick layer of fine-to-medium-grained quartzite. The quartzites from Rio do Ouro formation differ from the ones from Serra do Córrego Formation, on the high purity and the presence of preserved sedimentary structures. This unit marks the transition from a system of alluvial sedimentation to a shallow marine system dominated by tidal processes (Teles et al, 2015).

The Serra da Paciência Formation is exposed along the eastern margin of the Jacobina Basin and consists of thick packages of fine-to-coarse-grained quartzite, conglomeratic quartzites, and subordinate metaconglomerates, with contributions of blue quartz grains, possibly of volcanic origin (Pearson et al.,2005).

Meta-ultramafic and meta-mafic dykes and sills intersect all these units and mark the valleys at Jacobina Range. Veins of quartz-rich sulfides and gold are associated with

these rocks, which produced contact metamorphism in the surrounding metasedimentary rocks (Leo et al., 1964; Milesi et al., 2002; Pearson et al., 2005; Reis et al., 2021).

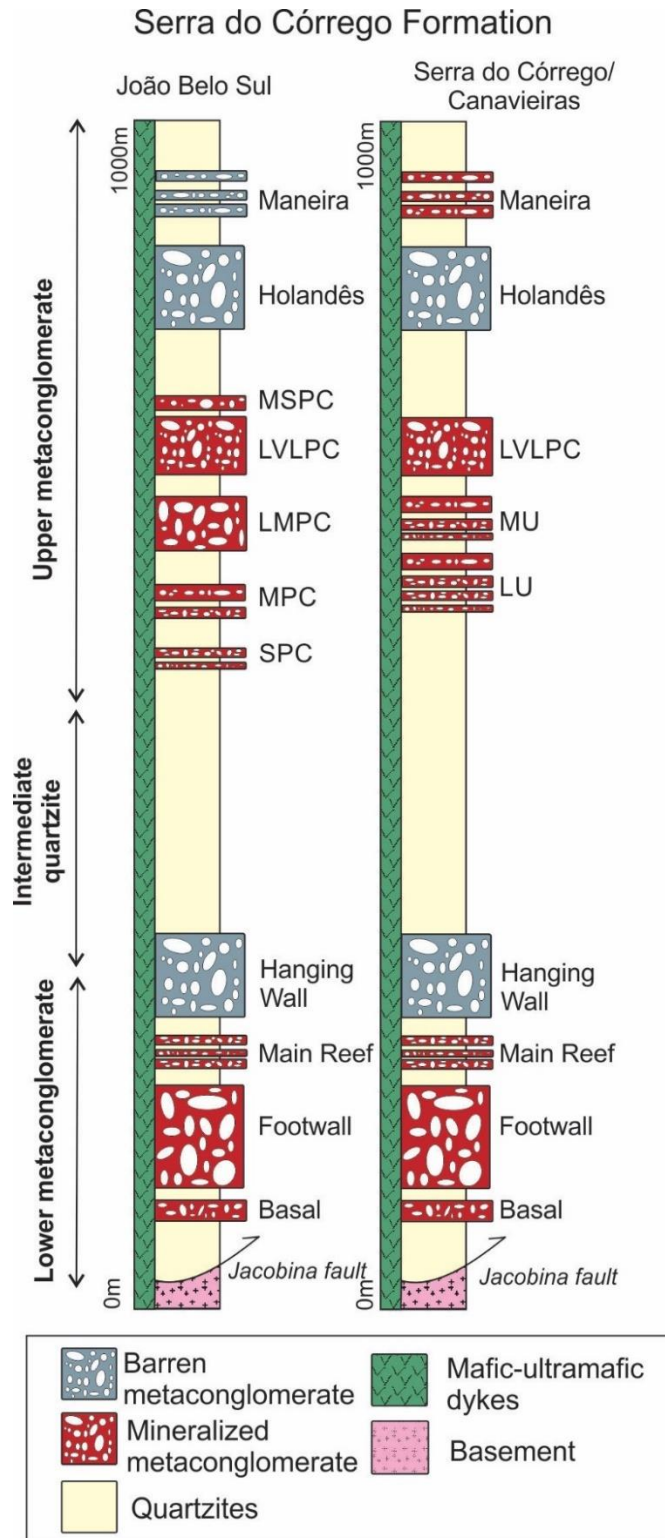


Fig. 2.3 Stratigraphic column of the Serra do Córrego Formation, Jacobina Group, for the João Belo Sul and Canaveiras/Serra do Córrego targets. In this column, the subunits (reefs) are color-coded based on whether the metaconglomerates are mineralized or barren. Modified after Teles et al. (2015).

2.3 Gold Mineralization

The gold-bearing metaconglomerates within the Serra do Córrego Formation have been subject to continuous mining activities since the 18th century by artisanal miners and, since 1983, by mining companies. Gold production in the Jacobina region continues to thrive, with five active mines contributing to this success: João Belo Norte, Morro do Vento Sul, Morro do Vento Central, Canavieiras Sul, and Canavieiras Central. Collectively, these mines achieved a remarkable production of 195,000 ounces in 2022, as reported by Yamana Gold (2023).

The Jacobina gold district displays a stratabound behavior and the targets show different mineralized layers. For the lower metaconglomerate zone the principal mineralized layers are Main Reef, Footwall and Basal reef and for the upper metaconglomerates the reefs Maneira, LVLPC, LMPC, MU and LU are the most economic ones (Fig. 2.3). The average grade varies between each target. Among all of them, the Canavieiras mine stand out as exhibits the highest grades. Pearson et al. (2005) linked this phenomenon to the interaction of the metaconglomerates with mafic-ultramafic bodies that were emplaced along north-trending structures. This interaction would provide fluid to the system, leading to the remobilization of gold and the formation of high-grade zones. Attesting to the importance of hydrothermal mineralization in forming this deposit.

The primary gold mineralization within the Serra do Córrego Formation is found in the matrix, surrounding quartz-pebbles, and along fractures and faults in the metaconglomerates (Fig. 2.5). Mineralized quartzite is not uncommon, however, they are mainly restricted to fracture and fault zones. Furthermore, the presence of mineralized meta-ultramafic and meta-mafic rocks intersecting with the Serra do Córrego Formation adds to the mineralization potential, often exhibiting favorable grades.

The origin of gold within the Jacobina basin has been a subject of extensive debate. Initially, it was classified as a classical paleoplacer deposit, drawing comparisons to the Archean Witwatersrand deposit in South Africa (Bateman, 1958). However, over time, various authors have emphasized the role of hydrothermal activity in the formation of gold mineralization in Jacobina. While some authors argue for a pure hydrothermal origin (Ledru et al., 1997; Milési et al., 2002; Pearson et al., 2005), the most widely accepted model is the "modified placer model" (Gross, 1968). According to this model, the primary placer mineralization was followed by ore mobilization through later

hydrothermal fluids (Robb and Meyer, 1991; Frimmel et al., 1993, 2019; Teles et al., 2015, 2020; Garayp and Frimmel, 2023).

3. Material and Methods

3.1 Sampling and Geochemical Data

The study area comprises the João Belo Sul, Serra do Córrego e Canavieiras targets, spaced 8km along the NS trend of the Jacobina mountain range. The main idea is to compare the geochemical signature, observing whether there is any relationship between bodies that exhibit higher grades and, also, to compare the influence of their geographic position along the basin. We selected 15 drill cores that intersect the complete sequence of the mineralized zone from the upper metaconglomerate and sampled at every 50 cm.

A total of 3048 drill core samples of metaconglomerate rocks (Maneira reef, Holandês reef, LVLPC reef, LMPC reef, MPC reef, MU reef, LU reef) were analysed for their major, minor and trace-element chemical composition. Multi-element assays using four-acid digest were produced by inductively coupled plasma mass spectrometry (ICP-MS) at ALS Laboratory, Vespasiano, Brazil, following the ME-MS61 procedure. The ICP-MS dataset contains 48 elements Ag, Al, As, Ba, Be, Bi, Ca, Cd, Ce, Co, Cr, Cs, Cu, Fe, Ga, Ge, Hf, In, K, La, Li, Mg, Mn, Mo, Na, Nb, Ni, P, Pb, Rb, Re, S, Sb, Sc, Se, Sn, Sr, Ta, Te, Th, Ti, Tl, U, V, W, Y, Zn, Zr. Gold was analyzed by fire assay. The raw database can be found in Appendix Table A1.

Also, we used optical microscopy to describe mineral assemblages and rock texture from the mineralized zones. Drill core samples from the João Belo Sul target and hand samples from underground galleries of Canavieiras were collected to produce polished thin sections. For João Belo Sul we selected samples from a mineralized and a barren drillcore to compare the reefs LVLPC and LMPC. Hand samples from Canavieiras came from high grade zones in reefs MU and LU.

3.2 Statistical analysis

In this paper, we followed the recommendations for dealing with compositional data proposed by Martín-Fernández et al. (2012), Buccianti and Grunsky (2014), and Gazley et al. (2015). To address elements with low concentrations that could not be detected, we applied a replacement method using 65% of the limit of detection (LOD).

This approach is suitable when less than 10% of the samples for the element of interest exhibit values below the LOD. If >30% of the samples for a given element is below LOD, that element must be discarded. Here, the elements Be, Ca, Cd, Ge, In, Re, Se, Sn, Ta and Tl were excluded for being below the LOD.

Compositional data are typically expressed as "closed" data, meaning they represent parts of a whole and thus exhibit intrinsic correlations with each other. Handling raw compositional data can lead to misinterpretations, primarily due to their strict positivity and constant sum constraint (Filzmoser et al., 2009; Zuo et al., 2013). This means that when one value changes, the others must also change to maintain the proportion. To address this challenge, log-ratio transformation techniques introduced by Aitchison (1982) have been adopted. These transformations create a new sample space with positive and negative values, allowing the application of classical statistics and therefore better interpretation of the relationships and patterns within geochemical data. Ensuring that the dataset conforms to a normal distribution is a crucial step for attesting the reliability of outcomes.

Here, centered log ratio (CLR) transform was applied to the raw dataset. CLR transform is calculated based on the geometric mean of the variables within a dataset. For that reason, it is necessary to have a complete dataset, meaning, the number of samples of each variable must be the same. The CLR-transformed database can be found in Appendix Table A1.

From the CLR-transformed data, boxplot diagrams (Tukey, 1977) were employed for an initial analysis of the geochemical background of the upper metaconglomerates in the João Belo Sul, Canavieiras, and Serra do Córrego targets. This approach provides a graphical data summary and is commonly used to distinguish the range that defines background values from anomalous values (Reimann et al., 2005). It is also an ideal alternative to compare different data subsets, as it graphically displays central tendency values and data dispersion for each subset.

Principal component analysis was used to produce geochemical groups within the upper metaconglomerate unit. PCA is a widely recognized multivariate analysis technique that finds extensive application in handling multidimensional datasets. Its primary advantage lies in its ability to reduce the dimensionality of data while retaining essential information from the original dataset (Jolliffe and Cadima, 2016). PCA operates by creating new artificial variables derived from a correlation matrix that captures most

of the variance present in the dataset and are uncorrelated to each other. These newly generated variables, known as principal components (PCs), can be visualized in a 2D diagram, aligning themselves along the directions of maximum variance within the data, where the first PC is the greatest variance, the second PC is the second greatest, and so on. The sum of the percentage contribution of each PC for the data variance is a fundamental tool to assess the quality of data dimension reduction, even though, the emphasis in PCA is almost always on the first PCs (Jolliffe and Cadima, 2016).

In this study all the geochemical data pre-processing, CLR transform and PCA were carried out using ioGAS™.

3.3 Unsupervised machine learning

Machine learning (ML), a subfield of artificial intelligence (AI), offers automated methods for uncovering patterns within complex datasets, empowering computers to learn and predict outcomes based on trained models (Liu, 2023). ML has witnessed significant adoption in geosciences, owing to its capacity to analyze vast datasets and discern intricate patterns (Caté et al., 2017). This technology finds diverse applications in geosciences, such as: geophysics, remote sensing, and geochemistry (Chen et al., 2020)

ML algorithms have become widely utilized for the identification of geochemical anomalies, mainly because geochemical analysis generates high-dimensional datasets with intricate relationships in non-2D or 3D spaces. This complexity poses a significant challenge in identifying patterns and making meaningful interpretations. To address this, unsupervised methods like self-organizing maps (SOM) have been effectively applied to identify geochemical patterns associated with mineralization.

Also, comparing different methods is a valuable practice in the geochemical pattern recognition process (Zuo, 2021). In this context, we decided to work with self-organizing maps (SOM) (Kohonen, 1990, 1997), a type of neural network, that works with data dimension reduction and clustering. Like other neural network, SOM, works with an input and an output layer, in the output layer neurons are interconnected representing a specific region of the input space (Gouvêa et al., 2023). Its greater advantage is preserving the topological structures of input data on the projected output space.

In SOM, every data item is mapped into one point (node) in the map, and the distances of the items in the map reflect similarities between them (Kohonen, 2013). The

number of neurons (M) in the output layer can be determined using a heuristic rule (Vesanto and Alhoniemi, 2000), where N is the number of input variables (1).

$$M = 5\sqrt{N} \quad (1)$$

SOM proves to be an excellent visualization tool as it provides U-matrix plot and component planes for each attribute in the dataset. The U-Matrix is essentially a topographic map of the SOM grid. It visually highlights the regions of the grid where data points are more similar (low distances) and where they are more dissimilar (high distances). Together with component planes it provides an intuitive visualization of the relationships and spatial arrangement of the dataset. We used IntraSOM, a Python library that implements Self-Organizing Maps with hexagonal toroidal maps training (Gouvêa et al., 2023).

4. Results

4.1 Field aspects and petrography of Serra do Córrego Formation Upper Metaconglomerate

The upper metaconglomerate from Serra do Córrego Formation displays similar macroscopic aspects throughout the entire Jacobina Gold District. However, stratigraphical differences between the sub-units (reefs) from João Belo Sul target and both Canavieiras and Serra do Córrego led the industry to adopt different names for these reefs in each target. Here, we follow the same nomenclature proposed by the industry and used by previous authors.

At the João Belo Sul target, the package of upper metaconglomerates has an average thickness of 480m and is composed, from the base to the top, of SPC, MPC, LMPC, LVLPC, MSPC (rare), Holândes, and Maneira reefs (Fig. 2.3). These metaconglomerates manifest as thick and continuous layers and they are, generally, grain supported with a pervasive oxidation alteration. The macroscopic description of the mineralized reefs in this target is summarized in Table 2.1.

Table. 2.2 Macroscopic description of the mineralized zone in the upper metaconglomerate at João Belo Sul target. The first column show photographs depicting typical samples from the corresponding reef, sourced from various drillholes. The second column provides a summarized description of each sub-unit.


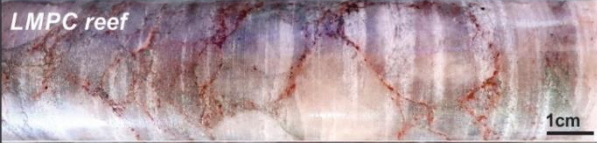


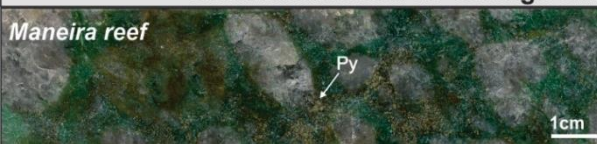



João Belo Sul mineralized zone macroscopic description	
 <p>LVLPC reef</p>	<p>LVLPC (Large - very large pebble conglomerate) Grain supported metaconglomerate with dominant pebble size varying from 3.2 - 6.4 cm and subordinated pebble > 6.4cm. Pebbles are mainly composed of milky quartz. Iron oxide and fuchsite alteration can be moderate to intense.</p>
 <p>LMPC reef</p>	<p>LMPC (Large - medium pebble conglomerate) Grain supported metaconglomerate with dominant pebble size varying from 3.2 - 6.4 cm and subordinated pebble size between 1.6 - 3.2 cm. Pebbles are composed of quartz. Intense iron oxide alteration.</p>
 <p>MPC reef</p> <p>Py</p>	<p>MPC (Medium pebble conglomerate) Grain supported metaconglomerate with dominant pebble size varying from 3.2 - 6.4 cm. Pebbles are composed of quartz. Intense iron oxide alteration locally associated with fuchsite-pyrite alteration.</p>
 <p>SPC reef</p> <p>Chert pebble</p>	<p>SPC (Small pebble conglomerate) Matrix supported metaconglomerate with dominant pebble size varying from 0.4 - 1.6 cm. Pebbles are composed of quartz and chert. Intense fuchsite-pyrite alteration.</p>

Table. 2.3 Macroscopic description of the mineralized zone in the upper metaconglomerate at Canavieiras and Serra do Córrego targets. The first column features photographs depicting typical samples from the corresponding reef, all obtained from drillholes in Canavieiras. Samples of LVLPC, MU, and LU reefs are derived from the same drillhole. The second column provides a concise summary of each sub-unit.

Canavieiras/Serra do Córrego mineralized zone macroscopic description	
 <p>Maneira reef</p> <p>Py</p>	<p>Maneira Reef Grain supported metaconglomerate, poorly sorted, pebbles can vary from 1.6 - 6.4 cm. Pebbles are mainly composed of milky quartz. Fuchsite alteration is intense and oxidation less frequent. This package is strongly intercalated with metric quartzite layers.</p>
 <p>LVLPC reef</p>	<p>LVLPC (Large - very large pebble conglomerate) Thick layer of grain supported metaconglomerate with dominant pebble size vary from 3.2 - 6.4 cm and subordinated pebble > 6.4cm. Pebbles are mainly composed of milky quartz. Iron oxide and fuchsite alteration can be moderate to intense with associated pyrite.</p>
 <p>MU reef</p>	<p>MU reef Grain supported metaconglomerate pebble size varying from 1.6 - 3.2 cm. Pebbles are mainly composed of milky quartz. Iron oxide and fuchsite alteration can be moderate to intense. Metaconglomerate layers are strongly intercalated with centimetric quartzite.</p>
 <p>LU reef</p>	<p>LU reef Grain supported metaconglomerate pebble size varying from 1.6 - 3.2 cm. Pebbles are mainly composed of milky quartz and chert. Intense fuchsite-pyrite alteration, often with chlorite associated. Metaconglomerate layers are moderate intercalated with quartzite.</p>

The upper metaconglomerates of the Canavieiras and Serra do Córrego targets exhibit macroscopic characteristics similar to the one from João Belo Sul, but differ in unit thickness, which is approximately 200m. Additionally, the metaconglomerate intervals are less continuous, with numerous intercalations of quartzite levels. To better illustrate these rocks, table 2.2 summarizes the macroscopic description of the mineralized reefs at both targets.

The petrographic analysis of the upper metaconglomerates from the João Belo Sul and Canavieiras targets has also shown that both exhibit similar textural and mineralogical characteristics (Fig. 2.5). The metaconglomerates are generally monomictic to oligomictic, most clasts consisting of quartz pebbles. The occurrence of chert clasts is common but represents less than 3% of the pebble type. Regarding the matrix, it comprises $\geq 85\%$ of strongly recrystallized quartz. The remaining minerals constituting the matrix include iron oxide-hydroxides -hematite and goethite- (5-15%), fuchsite (5-10%), and pyrite (<8%).

Fuchsite occurs as euhedral crystals in the matrix, around quartz pebbles and it is frequently associated with pyrite. In matrix-supported samples, the association of fuchsite and pyrite gently marks the foliation. For the João Belo Sul target, Fe-oxide alteration is very pervasive, it occurs in two main ways, as pyrite pseudomorphs or as small anhedral hematite crystals. The same alteration is significantly less intense in samples from Canavieiras.

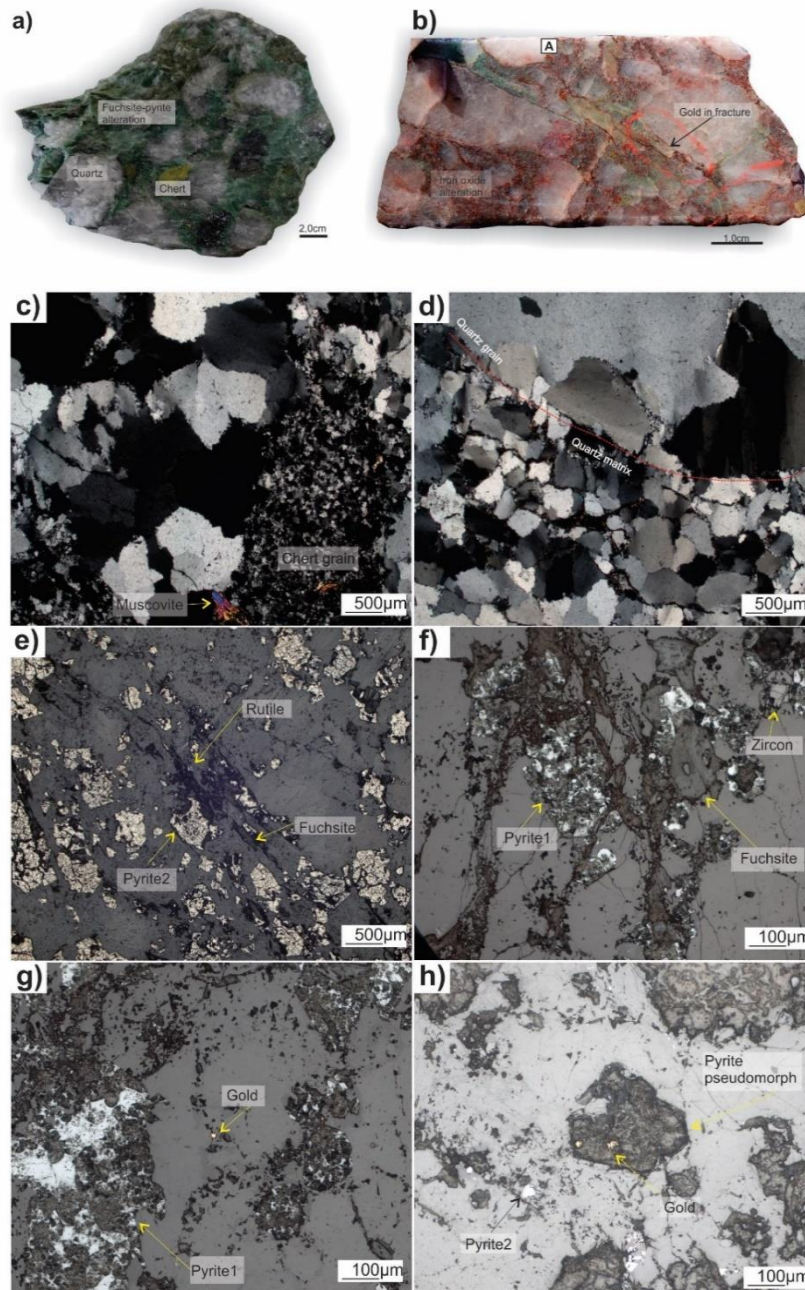


Fig. 2.4. Mineralized metaconglomerate samples and photomicrographs: a) Metaconglomerate sample from LVL reef in Canavieiras mine, well-packed metaconglomerate with quartz and chert pebbles and matrix with intense fuchsite-pyrite alteration. b) Drill core sample from LU reef from Serra do Córrego, well-packed metaconglomerate, with intense Fe-oxide alteration and visible gold hosted in fracture. c) and d) Oligomitic (clasts of quartz and chert) metaconglomerate photomicrograph (transmitted polarized light). e) subhedral epigenetic pyrite (Pyrite2) grains associated with fuchsite and rutile marking the foliation. f) Anedral sedimentary pyrite (Pyrite1) strongly altered to Fe-oxide with fuchsite associated and zircon. g) Rounded gold particle in metaconglomerate matrix with anedral pyrite grains. h) Gold included in pyrite pseudomorph. All photomicrographs are of samples from João Belo Sul, except “e”, which is from Canavieiras.

Two distinct groups of pyrites can be distinguished. The first group (pyrite1), associated with sedimentary processes, consists of rounded and anhedral pyrites exhibiting a pronounced Fe-oxide alteration. The oxidation process in pyrites from this

group is so intense that Fe-oxide minerals are observable as pseudomorphs of pyrite. The second group (pyrite₂) comprises epigenetic pyrites, varying in color from white to light-yellow, with crystals displaying subhedral to euhedral characteristics.

Sedimentary pyrite predominates in samples from João Belo Sul, characterized by its distinctive anhedral morphology and notable Fe-oxide alteration. While metaconglomerate samples from Canavieiras exhibit an abundance of epigenetic pyrite, showcasing crystals with a range of colors and predominantly subhedral to euhedral forms.

Even though samples were collected in mineralized zones, finding gold in thin sections is a challenge (Fig. 2.5). Gold displays irregular or rounded shapes, it is very thin and it is found associated with pyrites or in the matrix around quartz pebbles (Fig. 2.4e and 2.4g). Other opaque accessory minerals are rutile, chalcopyrite, zircon and chromite.

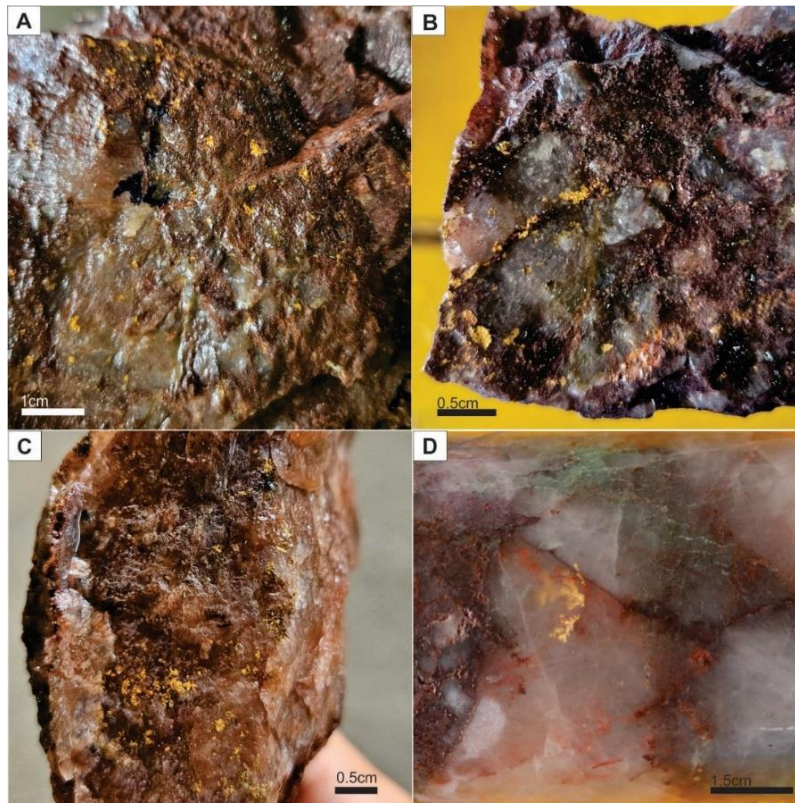


Fig. 2.5. Metaconglomerate samples with visible gold from Jacobina Gold District. A) Gold particles distributed along fracture in sample from LU reef – Canavieiras target; B) Visible gold around quartz pebbles in metaconglomerate sample from MU reef – Canavieiras target; C) Fracture plane with visible gold particles in sample from Main Reef; D) Large dendritic gold particle intercepted in a sample from a drillhole in the Footwall zone.

4.2 Whole rock geochemistry

In this study, the CLR-transformed dataset was utilized to produce box plots of selected elements - Au, Ag, As, Bi, Cr, Cu, Fe, Mg, Ni, S, Sc, Th, U, and Zr (Fig. 2.6). The elements were selected aiming to test the differences between the geochemical background of the targets based on the gold mineralization and the influence of hydrothermal fluids. The diagrams are combined for the three targets. Each box is colored representing one of the targets and inside the box the black line is the median value and the black dot is the mean.

As mentioned previously, Canavieiras target has the highest mean content of gold and has a higher mafic contribution, as can be seen by higher values of Mg and Ni and the abundance of mafic-ultramafic dykes intercepting this target. The calcophile elements, Ag, As, Bi and Cu are higher for the João Belo Sul target and so are the lithophiles, Sc, Th, U and Zr. The Serra do Córrego target shows lower values for all the elements when compared to the other targets.

Correlation matrices for each target were produced to help underlying geochemical patterns. Positive and negative correlations within the three targets varies between moderate ($r > 0.4$) and very weak ($r > 0.1$). Higher correlation indexes, ($r > 0.5$) occur locally.

In the correlation matrix for João Belo Sul (Table 2.3), we observe moderate correlations within the associations of Au-As-Fe-Sb-Te and Co-Cr-Cu-Ni-S-U-Zn. Additionally, a strong ($r > 0.5$) negative correlation is identified for As(-Mg-Ti). Similar correlations are present in the Serra do Córrego dataset, ranging from moderate to weak. However, the Canavieiras dataset displays a distinct pattern, featuring a weak correlation between As-S-Sb-Sr, but in contrast, a strong positive correlation emerges in the association of Mg-Ni-Zn.

When comparing the correlation matrix of the CLR-transformed dataset to that of the raw dataset, there is minimal disparity. The element associations remain consistent in both matrices. However, the correlation indices are noticeably attenuated when using the raw dataset. For example, moderate correlation indexes ($0.5 > r$) in the CLR-transformed dataset become very weak or non-existent in the raw dataset.

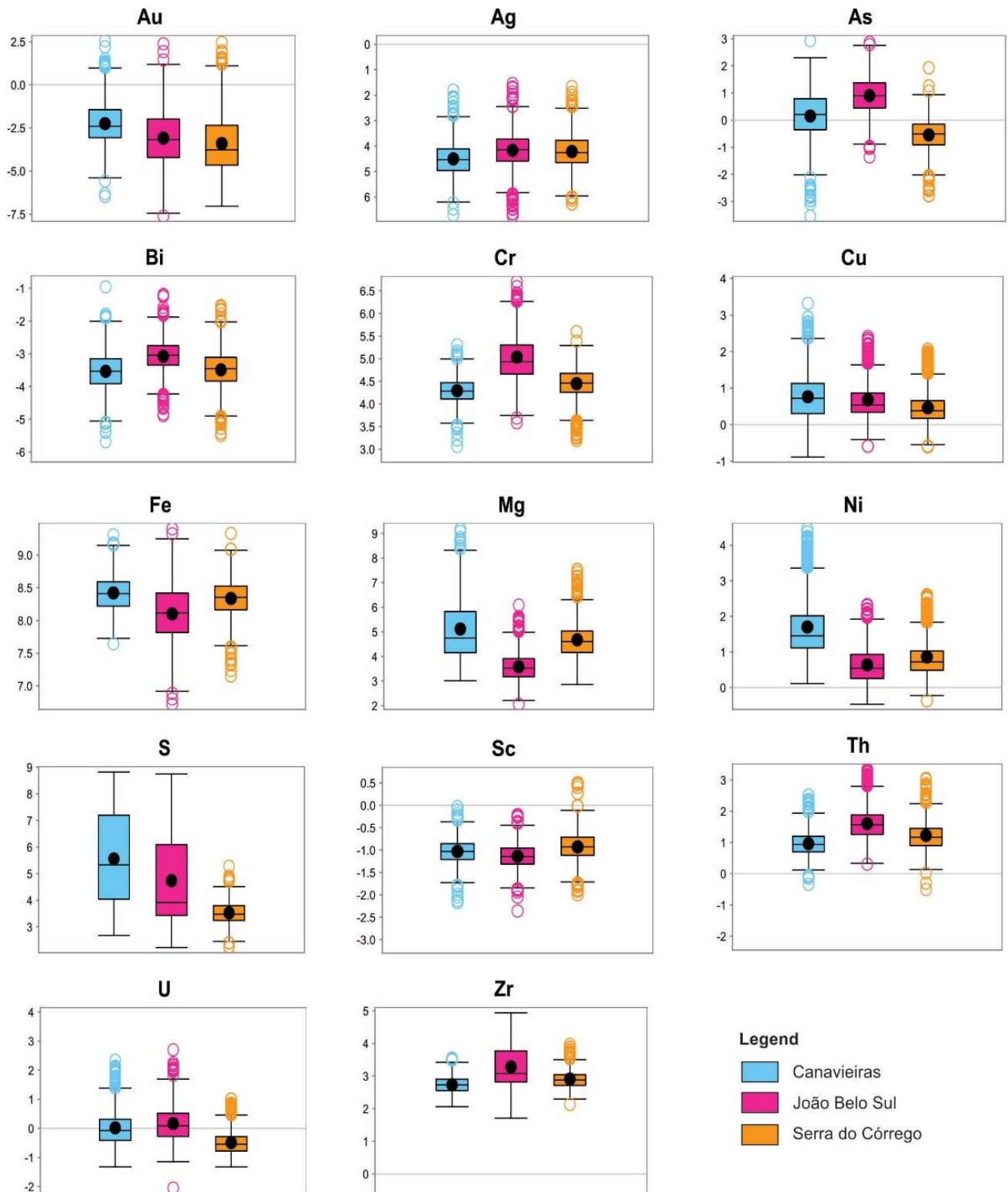


Fig. 2.6. Box and whisker plots of selected elements (Au, Ag, As, Bi, Cr, Cu, Fe, Mg, Ni, S, Sc, Th, U and Zr). The circles beyond the limit of the whiskers are outlier samples. Diagrams for the other elements in the dataset can be accessed in the appendix.

Table. 2.4 Correlation matrix of selected elements from the João Belo Sul dataset. The correlation matrices for Canavieiras and Serra do Córrego can be found in Appendix Table A2.

	Au	Ag	As	Bi	Co	Cr	Cu	Fe	Mo	Mg	Ni	Pb	S	Sb	Sr	Te	Ti	U	Zn
Au	1.00	0.36	0.47	0.10	-0.17	-0.16	0.00	0.41	0.22	-0.36	-0.13	0.25	0.00	0.53	0.23	0.44	-0.43	-0.03	-0.34
Ag	0.36	1.00	0.08	-0.19	-0.29	-0.33	-0.05	0.10	0.19	-0.08	-0.04	0.01	0.00	0.27	-0.02	0.18	-0.18	-0.20	-0.30
As	0.47	0.08	1.00	0.20	0.28	0.04	0.15	0.53	0.04	-0.52	0.33	0.27	0.52	0.46	0.22	0.31	-0.63	0.36	-0.35
Bi	0.10	-0.19	0.20	1.00	0.31	0.34	0.25	0.09	-0.22	-0.21	-0.02	0.14	0.08	0.13	0.19	0.34	-0.25	0.32	0.24
Co	-0.17	-0.29	0.28	0.31	1.00	0.61	0.49	0.03	-0.35	-0.25	0.54	-0.34	0.63	-0.27	-0.38	-0.22	-0.41	0.61	0.47
Cr	-0.16	-0.33	0.04	0.34	0.61	1.00	0.32	0.05	-0.32	-0.32	0.02	-0.29	0.12	-0.16	-0.16	-0.14	-0.18	0.40	0.62
Cu	0.00	-0.05	0.15	0.25	0.49	0.32	1.00	0.10	-0.19	-0.21	0.34	-0.08	0.32	-0.03	-0.23	-0.10	-0.35	0.51	0.17
Fe	0.41	0.10	0.53	0.09	0.03	0.05	0.10	1.00	0.06	-0.28	0.04	-0.01	0.10	0.49	0.06	0.21	-0.37	-0.04	-0.23
Mo	0.22	0.19	0.04	-0.22	-0.35	-0.32	-0.19	0.06	1.00	-0.01	0.13	0.05	0.02	0.20	-0.01	0.06	-0.03	-0.24	-0.32
Mg	-0.36	-0.08	-0.52	-0.21	-0.25	-0.32	-0.21	-0.28	-0.01	1.00	-0.05	-0.24	-0.23	-0.32	-0.21	-0.19	0.49	-0.41	0.03
Ni	-0.13	-0.04	0.33	-0.02	0.54	0.02	0.34	0.04	0.13	-0.05	1.00	-0.27	0.78	-0.19	-0.46	-0.23	-0.39	0.42	-0.07
Pb	0.25	0.01	0.27	0.14	-0.34	-0.29	-0.08	-0.01	0.05	-0.24	-0.27	1.00	-0.25	0.39	0.58	0.37	-0.07	0.16	-0.29
S	0.00	0.00	0.52	0.08	0.63	0.12	0.32	0.10	0.02	-0.23	0.78	-0.25	1.00	-0.10	-0.40	-0.18	-0.51	0.48	-0.11
Sb	0.53	0.27	0.46	0.13	-0.27	-0.16	-0.03	0.49	0.20	-0.32	-0.19	0.39	-0.10	1.00	0.31	0.54	-0.28	-0.15	-0.37
Sr	0.23	-0.02	0.22	0.19	-0.38	-0.16	-0.23	0.06	-0.01	-0.21	-0.46	0.58	-0.40	0.31	1.00	0.43	-0.05	-0.11	-0.19
Te	0.44	0.18	0.31	0.34	-0.22	-0.14	-0.10	0.21	0.06	-0.19	-0.23	0.37	-0.18	0.54	0.43	1.00	-0.23	-0.11	-0.16
Ti	-0.43	-0.18	-0.63	-0.25	-0.41	-0.18	-0.35	-0.37	-0.03	0.49	-0.39	-0.07	-0.51	-0.28	-0.05	-0.23	1.00	-0.37	-0.01
U	-0.03	-0.20	0.36	0.32	0.61	0.40	0.51	-0.04	-0.24	-0.41	0.42	0.16	0.48	-0.15	-0.11	-0.11	-0.37	1.00	0.12
Zn	-0.34	-0.30	-0.35	0.24	0.47	0.62	0.17	-0.23	-0.32	0.03	-0.07	-0.29	-0.11	-0.37	-0.19	-0.16	-0.01	0.12	1.00

4.3 Geochemical pattern in PCA space

4.3.1 Mapping local geochemical signature

We utilized the complete database comprising 3047 metaconglomerate samples clr-transformed from the three targets as the first step as input to the principal component analysis (PCA). The calculated values for the first two components—PC1 and PC2—account for 22.7% and 17.2% of the data variance, respectively. From the PC1-PC2 diagram, we plotted the samples classified according to each target, revealing the formation of three groups with distinct geochemical affinities (Fig. 2.7). Samples from João Belo Sul concentrate on the right portion of the diagram, indicating a higher correlation with U, As, Te, Bi, Sb, Pb, Cr, Th, Sr, Hf, Zr, and P. Metaconglomerates from Serra do Córrego are situated in the lower-left corner and are associated with Al, Na, Ti, Rb, K, Nb, and Sc. Lastly, the group of Canavieiras samples concentrates in the central top of the diagram and exhibits association with Z, Cu, Co, S, Au, Ni, Fe, Mo, Li, Mg, and Mn.

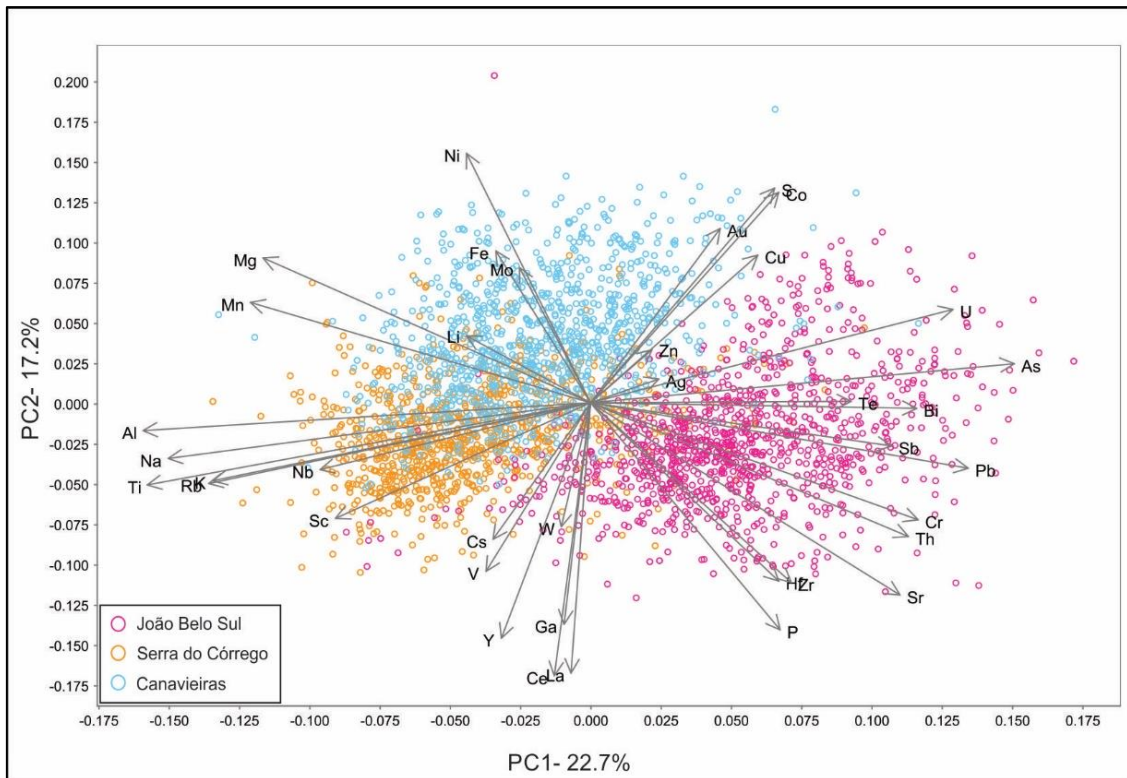


Fig. 2.7. Principal component analysis (PCA) biplot of the first two principal components. PC1 represents 22.7% of the variance and PC2 represents 17.2%. Metaconglomerate samples are colored according to the target.

4.3.2 Targeting gold mineralization signatures

PCA was also applied individually for each of the three targets. Our first approach was to apply PCA for the complete CLR-transformed dataset. Some geochemical associations related to gold mineralization were mapped. However, some elements (e.g. Al, K, Na, Hf and Zr) that have significant concentrations, but are not directly related to gold mineralization in the Jacobina context, end up masking other elements that besides having lower concentrations are more associated with gold. As a second approach we applied PCA for selected elements – Au, Ag, As, Bi, Co, Cr, Cu, Fe, Ga, Mo, Mg, Ni, Pb, S, Sb, Sc, Sr, Te, Th, Ti, U and Zn. With this approach elements association became easily visualized. The PCA calculation for the three targets can be found in Appendix Table A2.

Table 2.4 summarizes the relative contribution of each PC for target. To select the most significant PCs we used scree plots. A scree plot is a graphic representation of the eigenvalue of each PC. The idea of a scree plot is to look for the “elbow” in the curve and select the PCs before the line flattens out. The PCs whose eigenvalues were above 1, were selected as most representative of data variability. For Canavieiras six PCs were selected

and they account of 71.38% of data variability. For João Belo Sul and Serra do Córrego five PCs account of 69.14% and 61.95% of variability, respectively.

Table 2.5. Table of selected principal components representing the biggest data variability for each target, calculated from transformed geochemical data ($n_{\text{João Belo Sul}} = 1110$ samples; $n_{\text{Canavieiras}} = 1001$ samples; $n_{\text{Serra do Córrego}} = 936$ samples).

	João Belo Sul			Canavieiras			Serra do Córrego		
	Eigenvalues	Percent	Cumulative %	Eigenvalues	Percent	Cumulative %	Eigenvalues	Percent	Cumulative %
PC1	4.98	22.65	22.65	5.26	23.93	23.93	5.25	23.88	23.88
PC2	4.47	20.31	42.97	4.15	18.86	42.79	3.21	14.61	38.49
PC3	2.86	12.99	55.95	2.19	9.95	52.74	2.15	9.79	48.28
PC4	1.70	7.72	63.67	1.76	8.02	60.76	1.59	7.23	55.52
PC5	1.20	5.47	69.14	1.29	5.88	66.64	1.42	6.44	61.95
PC6				1.04	4.73	71.38			

Following the same methodology employed by Hood et al. (2019), table 2.5 lists the contribution of each element to each PC. Elements with positive correlation are colored in red and elements with negative correlation are colored in blue. PC1-PC3 were used as axes to plot elements eigenvectors in 2D diagrams. Metaconglomerate samples are plotted together and are classified according to their average gold content, high grade (>5g/t), medium grade (5-2g/t), low grade (2-1g/t) and barren samples (<1g/t). This classification considers the economic value of mining in Jacobina's gold district.

It is evident in the 2D diagrams (Fig. 2.8) that there are geochemical associations directly related to gold mineralization for the three targets. Mineralized samples are concentrated in the direction of specific elements. Some barren samples are also plotted in the same field, but there is a clear separation between them and the mineralized ones. Although the samples are classified by grade variations, the principal component diagrams do not show any distinction between groups of samples with similar grades.

From the binary plot of PC1 vs. PC2 for the João Belo Sul target (Fig. 2.8A), we identify a well-marked cluster for the mineralized samples. The geochemical associations that delineate this cluster are as follows: (a) PC1, with a strong positive influence of the elements As, Au, Fe, S, Sb, U, and Bi; (b) PC2, with positive values for Sr, Sb, Te, Pb, Au, Ag, and Mo. A similar pattern is observed in the Serra do Córrego dataset (Fig. 2.8C), where the PC1 vs. PC2 biplot reveals the grouping of mineralized samples within a distinct cluster. This clustering results from the positive associations of As, Au, Te, Pb, U, Sr, Sb, Th, and Bi identified in PC1.

Unlike the first two targets, in the Canavieiras dataset, the PC1 vs. PC3 biplot reveals the presence of two clusters among the mineralized samples. One cluster is associated with the positive values of Th, Cr, Fe, Au, Pb, Ag, Bi, Te, U, and Mo identified in PC3 (Fig. 2.8B). The second cluster is characterized by the strong negative values of Mg, Zn, Ni, Ga, Ti, and Sc in PC1.

4.4 SOM clustering

The first attempt at clustering using SOM was made with the same dataset selected for PCA, which included 21 elements CLR-transformed. At this initial stage, we observed a high quantization error value, ranging from 3.1 to 3.5, which directly affected the map's resolution, resulting in poorly defined clusters with low contrast against the background. We considered that this error could be related to the fact that the chemical differences between the mineralized and barren samples are very subtle in Jacobina's gold district. So, we reviewed our dataset and using the results from PCA we excluded the elements that showed less correlation.

Table 2.6. Table of the scaled eigenvectors for the most representative PCs, each PC has been sorted individually so all the positive and negative correlations are displayed in order.

João Belo Sul										Canavieiras										Serra do Córrego											
PC1		PC2		PC3		PC4		PC5		PC1		PC2		PC3		PC4		PC5		PC6		PC1		PC2		PC3		PC4		PC5	
As	0.37	Sr	0.29	Mo	0.31	Zn	0.42	Fe	0.44	As	0.35	Co	0.42	Th	0.42	Mo	0.40	Ag	0.55	Pb	0.35	As	0.32	Ni	0.41	Mo	0.45	Sr	0.26	Ag	0.55
Au	0.26	Sb	0.29	Ni	0.28	Cr	0.23	Cr	0.37	Sb	0.34	U	0.37	Cr	0.40	Fe	0.37	Au	0.31	U	0.31	Au	0.31	Co	0.41	S	0.35	Ni	0.21	Cu	0.26
Fe	0.24	Te	0.26	Ag	0.26	Bi	0.19	Ga	0.31	Sr	0.33	S	0.32	Fe	0.38	Ag	0.24	Cu	0.12	Au	0.27	Te	0.29	Cu	0.36	Fe	0.23	Mg	0.12	S	0.23
S	0.23	Pb	0.26	S	0.26	Te	0.15	Sc	0.28	Bi	0.24	Cu	0.32	Au	0.36	Au	0.21	Te	0.11	Mo	0.27	Pb	0.29	Zn	0.27	Sb	0.15	As	0.12	U	0.20
Sb	0.22	Au	0.23	Mg	0.11	Fe	0.13	Sb	0.23	Te	0.23	Bi	0.25	Pb	0.32	Ni	0.17	Pb	0.07	Ti	0.21	U	0.27	Mg	0.27	Te	0.11	Mo	0.10	Au	0.17
U	0.21	Ag	0.18	Fe	0.11	Mg	0.12	As	0.15	S	0.19	Ni	0.18	Ag	0.21	Sb	0.13	Sr	0.06	S	0.13	Sr	0.23	Fe	0.22	Sr	0.05	U	0.09	Pb	0.15
Bi	0.20	Mo	0.16	Au	0.09	Ag	0.10	Au	0.13	Ag	0.09	Zn	0.16	Bi	0.18	Zn	0.11	Bi	0.01	As	0.05	Sb	0.22	Ag	0.21	Zn	0.04	Pb	0.09	Mo	0.12
Te	0.19	Th	0.10	As	0.05	Au	0.09	Zn	0.01	Mo	0.07	Mg	0.14	Te	0.17	Mg	0.08	Ti	0.01	Fe	0.01	Th	0.20	Mo	0.15	Ag	0.03	Au	0.09	Ti	0.09
Co	0.19	Fe	0.10	Sb	0.01	Co	0.04	Co	0.00	Cu	0.05	Pb	0.14	U	0.16	Te	0.00	Mg	-0.02	Sr	-0.01	Bi	0.18	Sb	0.14	Au	0.01	Ga	0.03	Bi	0.04
Cu	0.18	Ti	0.06	Co	-0.06	Sb	0.03	Ti	0.00	Pb	0.05	Au	0.13	Zn	0.12	Co	-0.02	Ga	-0.02	Ga	-0.02	Mo	0.10	Au	0.08	As	-0.01	Ag	0.02	Cr	0.04
Ni	0.15	As	0.04	Cu	-0.06	Cu	-0.03	Mo	-0.04	Cr	0.05	As	0.13	Mo	0.12	Cu	-0.04	Zn	-0.04	Ag	-0.04	Fe	0.09	S	0.06	Ga	-0.01	Th	-0.06	Th	0.03
Th	0.15	Mg	0.00	Ga	-0.07	Ti	-0.04	Sr	-0.07	Fe	0.04	Th	0.11	Sc	0.03	Bi	-0.04	Sc	-0.08	Zn	-0.07	Cr	0.09	Bi	0.03	Ti	-0.05	Cu	-0.07	Ga	0.03
Pb	0.10	Sc	-0.03	Ti	-0.08	Mo	-0.04	Cu	-0.08	U	0.03	Ag	0.03	Ni	0.03	S	-0.05	U	-0.08	Co	-0.11	Ag	0.07	U	0.00	Cr	-0.08	Zn	-0.08	Zn	-0.01
Cr	0.08	Ga	-0.05	Te	-0.14	Sr	-0.06	Ag	-0.08	Au	0.02	Te	-0.04	Ga	0.02	As	-0.06	Th	-0.09	Mg	-0.13	Co	0.00	Te	-0.02	Cu	-0.09	Sc	-0.12	Mg	-0.11
Ag	0.07	Bi	-0.06	U	-0.18	Th	-0.13	S	-0.09	Th	0.01	Cr	-0.07	Ti	0.02	Cr	-0.15	Ni	-0.13	Th	-0.13	S	-0.06	As	-0.03	Ni	-0.13	Te	-0.12	Te	-0.12
Sr	0.07	Cu	-0.23	Sc	-0.23	S	-0.22	U	-0.09	Co	-0.09	Sb	-0.07	Cu	-0.01	Sr	-0.15	Sb	-0.15	Cr	-0.15	Cu	-0.06	Pb	-0.03	Sc	-0.17	Sb	-0.13	Sc	-0.17
Mo	0.01	U	-0.25	Zn	-0.24	As	-0.23	Te	-0.16	Sc	-0.14	Fe	-0.13	Sb	-0.01	U	-0.22	As	-0.18	Sb	-0.17	Zn	-0.07	Th	-0.09	Pb	-0.19	Co	-0.14	As	-0.20
Zn	-0.06	Zn	-0.26	Pb	-0.25	Ni	-0.25	Pb	-0.16	Ti	-0.15	Mo	-0.15	Mg	-0.03	Ga	-0.23	S	-0.18	Cu	-0.21	Ni	-0.11	Cr	-0.15	Bi	-0.20	S	-0.23	Ni	-0.22
Sc	-0.23	S	-0.26	Cr	-0.26	Ga	-0.30	Ni	-0.21	Ga	-0.25	Ga	-0.22	Sr	-0.09	Sc	-0.26	Co	-0.21	Bi	-0.22	Mg	-0.28	Sc	-0.18	Mg	-0.24	Ti	-0.24	Co	-0.23
Mg	-0.28	Ni	-0.27	Sr	-0.28	U	-0.32	Bi	-0.21	Ni	-0.33	Sc	-0.23	Co	-0.15	Pb	-0.27	Fe	-0.30	Ni	-0.23	Sc	-0.28	Ga	-0.19	Co	-0.26	Fe	-0.34	Sb	-0.25
Ga	-0.33	Cr	-0.28	Bi	-0.30	Pb	-0.34	Th	-0.25	Zn	-0.35	Sr	-0.24	As	-0.15	Ti	-0.31	Cr	-0.37	Sc	-0.23	Ti	-0.28	Ti	-0.24	U	-0.32	Bi	-0.48	Sr	-0.27
Ti	-0.37	Co	-0.39	Th	-0.42	Sc	-0.40	Mg	-0.40	Mg	-0.37	Ti	-0.26	S	-0.27	Th	-0.38	Mo	-0.40	Te	-0.52	Ga	-0.33	Sr	-0.29	Th	-0.47	Cr	-0.54	Fe	-0.37

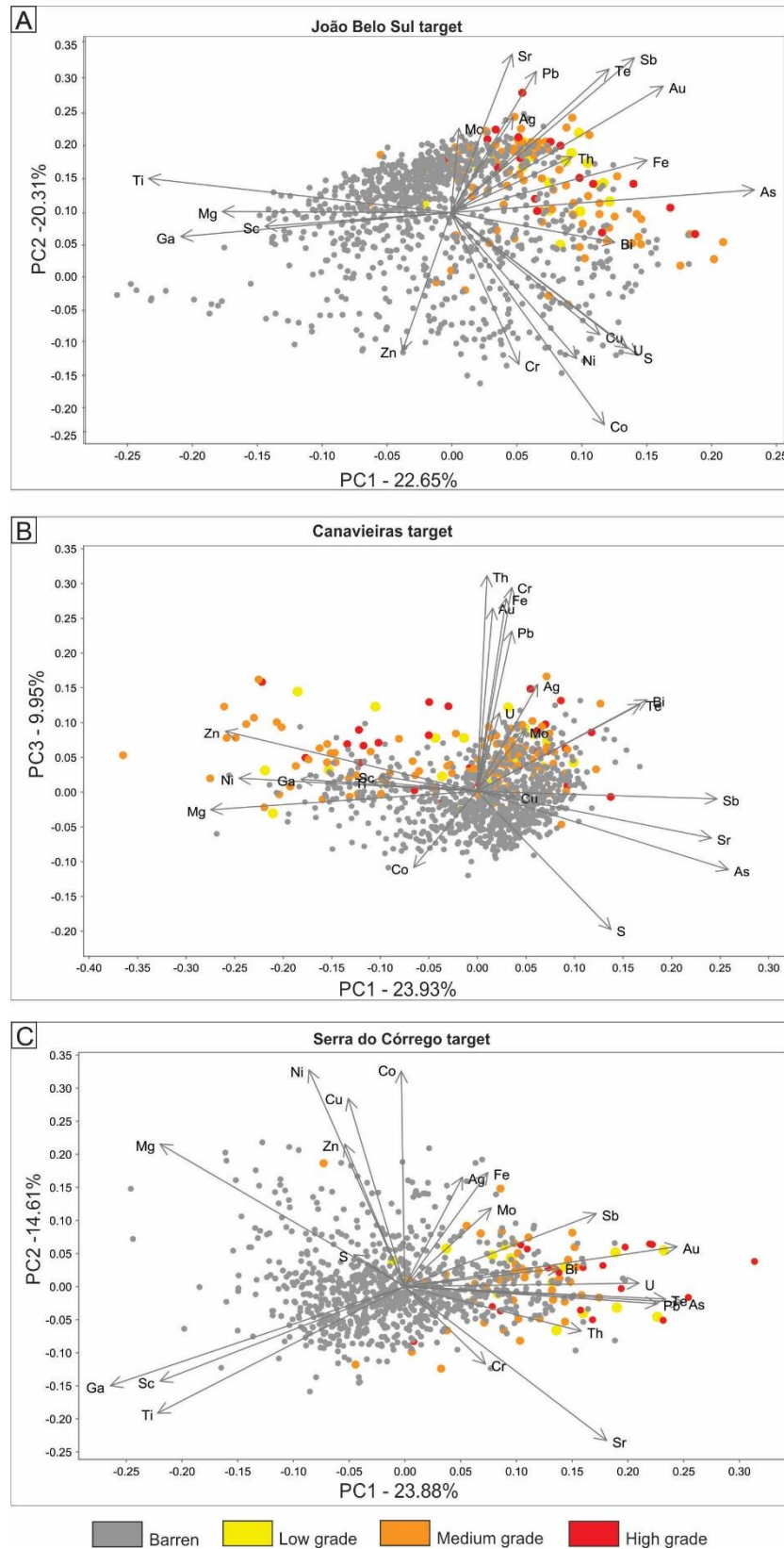


Fig. 2.8. Results of PCA plotted in a biplot with metaconglomerate samples colored according to the ore content. PCs were selected aiming to better display the mineralized clusters. (A) João Belo Sul PC1 vs. PC2 – mineralized samples are concentrated around the eigenvectors of Mo, Sr, Ag, Pb, Te, Sb, Au, Th, Fe, As and Bi; (B) Canaveiras plot of PC1 vs. PC3 – the samples are grouped into two areas of the diagram. The first marks the association with Au, Cr, Fe, Pb, U, Ag, Mo, Te and Bi. The second group

marks the association with Mg, Ni, Zn, Ga, Ti and Sc. (C) Serra do Córrego plot of PC1 vs. PC2 – mineralized samples group around the eigenvectors of As, Au, Te, Pb, U, Sr, Sb, Th, and Bi.

For our second attempt, we applied the SOM to a total of 17 elements - Ag, As, Au, Bi, Co, Cr, Cu, Fe, Mg, Mo, Ni, Pb, Sb, S, Te, U, and Zn. Just like for PCA, SOM was applied for each one of the three targets dataset. The quantization errors were reduced to about 2.7 to 3.0, which was sufficient to improve the visualization of the dissimilarity boundaries in the unified distance matrix (U-matrix) (Fig. 2.8). This representation allows assessing the relationships between the map neurons and its distributions in the dataset, by distinguishing regions with low dissimilarity, which are expected to form clusters.

The analysis of each U-matrix revealed a narrow and circular dissimilarity boundary in the Canavieiras target (Fig. 2.9A), while the João Belo Sul (Fig. 2.9B) and Serra do Córrego (Fig. 2.9C) targets presented more wide and sparse boundaries. Using the component plots it is possible to visualize the distribution of each element within the SOM space and to establish correlations among them (Fig. 2.10). The component plots display the values for the elements in each map neuron lots can be seen as a same grid applied for each element, where the element distribution varies from low to high. The geochemical associations are easily mapped by recognizing distribution patterns within the component plots.

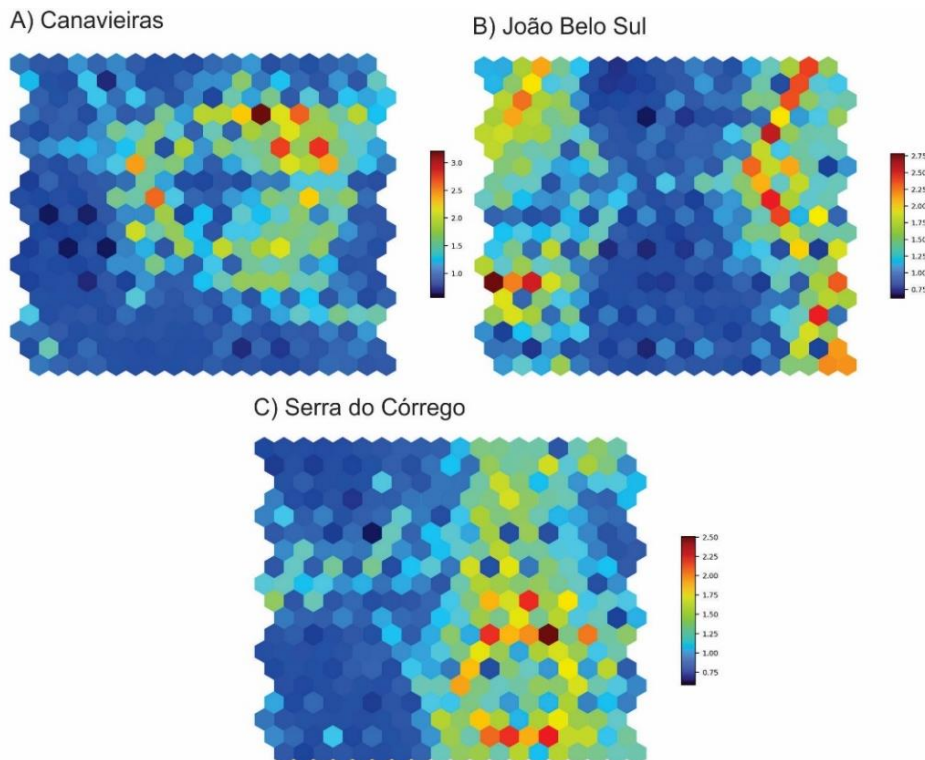
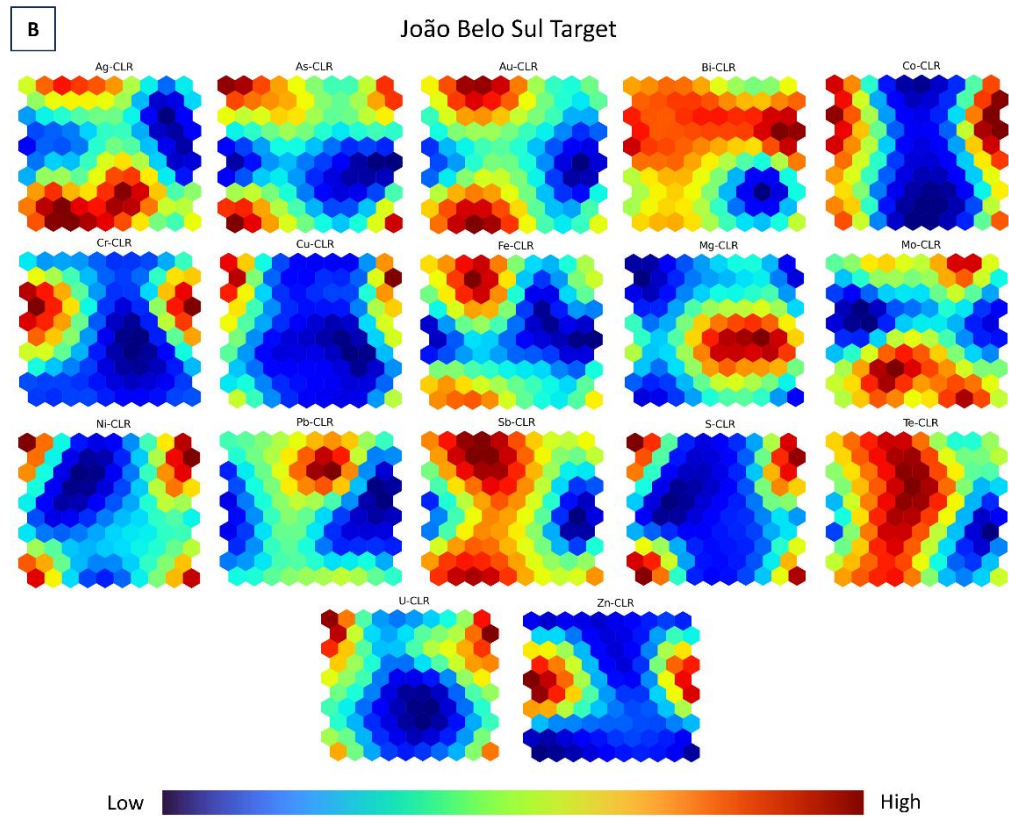
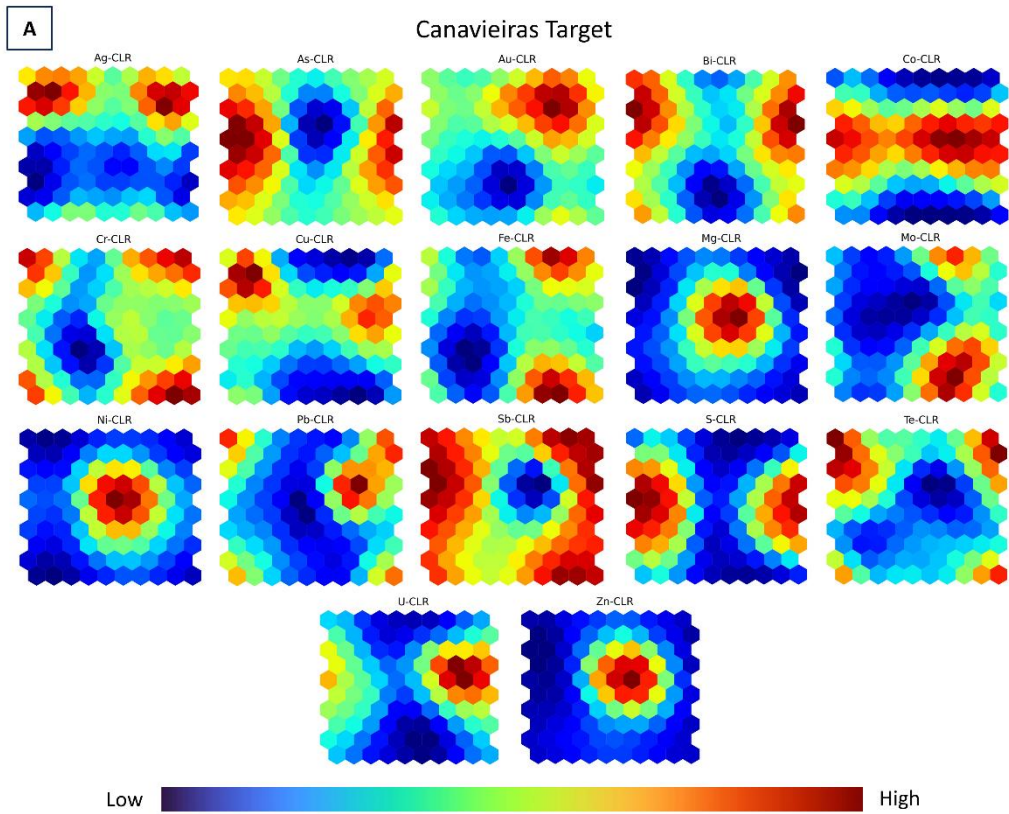


Fig. 2.9. Unified distance matrix (U-matrix) for each of the three datasets. Each neuron is colored representing the distance between the adjacent neurons. Warmer colors represent longer distances, mining more dissimilarity.



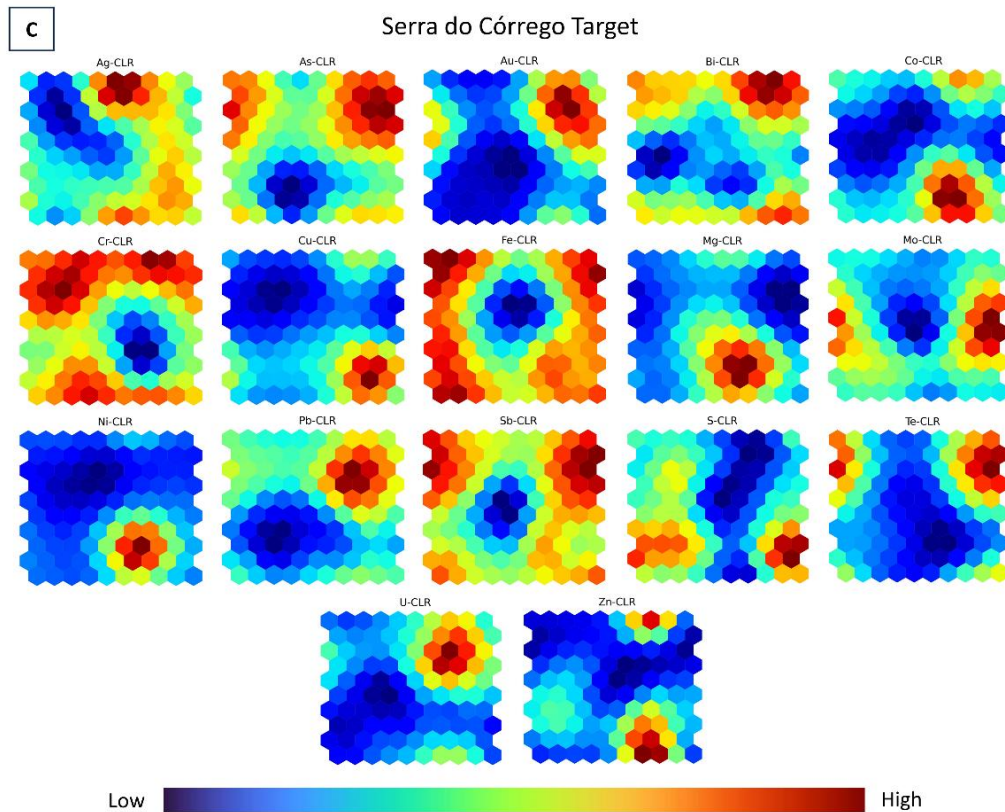


Fig. 2.10. Component planes of geochemical variables analyzed in self-organizing map (SOM) presented for each target - (A) Canaveira, (B) João Belo Sul and (C) Serra do Córrego.

For Canaveiras, Au, Ag, Bi, Cr, Fe, Pb, Sb, and Te exhibit a similar pattern with higher values concentrated in the top-right corner. Additionally, a notable cluster marked by high values of Mg, Ni, and Zn is evident in the central region of the plot (Fig. 2.10A). In João Belo Sul, higher gold values are prominently situated in the top and bottom left corners. Ag, As, Bi, Fe, Sb, and Te show strong associations, as high values are displayed in the same area (Fig. 2.10B). Lastly, when comparing the component plots for Serra do Córrego, an association of Au, As, Bi, Fe, Pb, Sb, and Te is apparent, with high values clustered in the top-right corner (Fig. 2.10C).

Following the approach of Chen et al. (2023), we superimposed SOM component plots to better investigate and define geochemical associations (Fig. 2.11). For each of the target areas, we were able to pinpoint the most substantial clusters, whether they were linked to Au mineralization or not. Each cluster is assigned a distinct color and is labeled according to its elemental association. By utilizing the color gradients in each component

plot, we were able to delineate higher values and create a unified plot that represents the distribution of all 17 elements within the SOM space.

Starting with Canavieiras, we identified nine distinct clusters. Among these, four are associated with Au mineralization (Au-Ag-Fe-Mo-Sb; Au-Ag-As-Bi-Pb-U; Au-Mg-Ni-Zn; Au only), and one represents a mafic correlation (Mg-Ni-Zn) (Fig. 2.11a). In the Serra do Córrego dataset, a similar mafic cluster is delineated (Mg-Ni-Zn), and only one cluster exhibits a correlation with gold (Au-As-Bi-Sb-Pb-Fe-Te) (Fig 2.11c). The João Belo Sul dataset stands out as it does not display any mafic associations. Instead, we identified two distinct clusters related to Au - Au-Ag-As-Fe-Sb-Te-Bi and Au-Ag-As-Fe-Sb-Te-Mo (Fig. 2.11b).

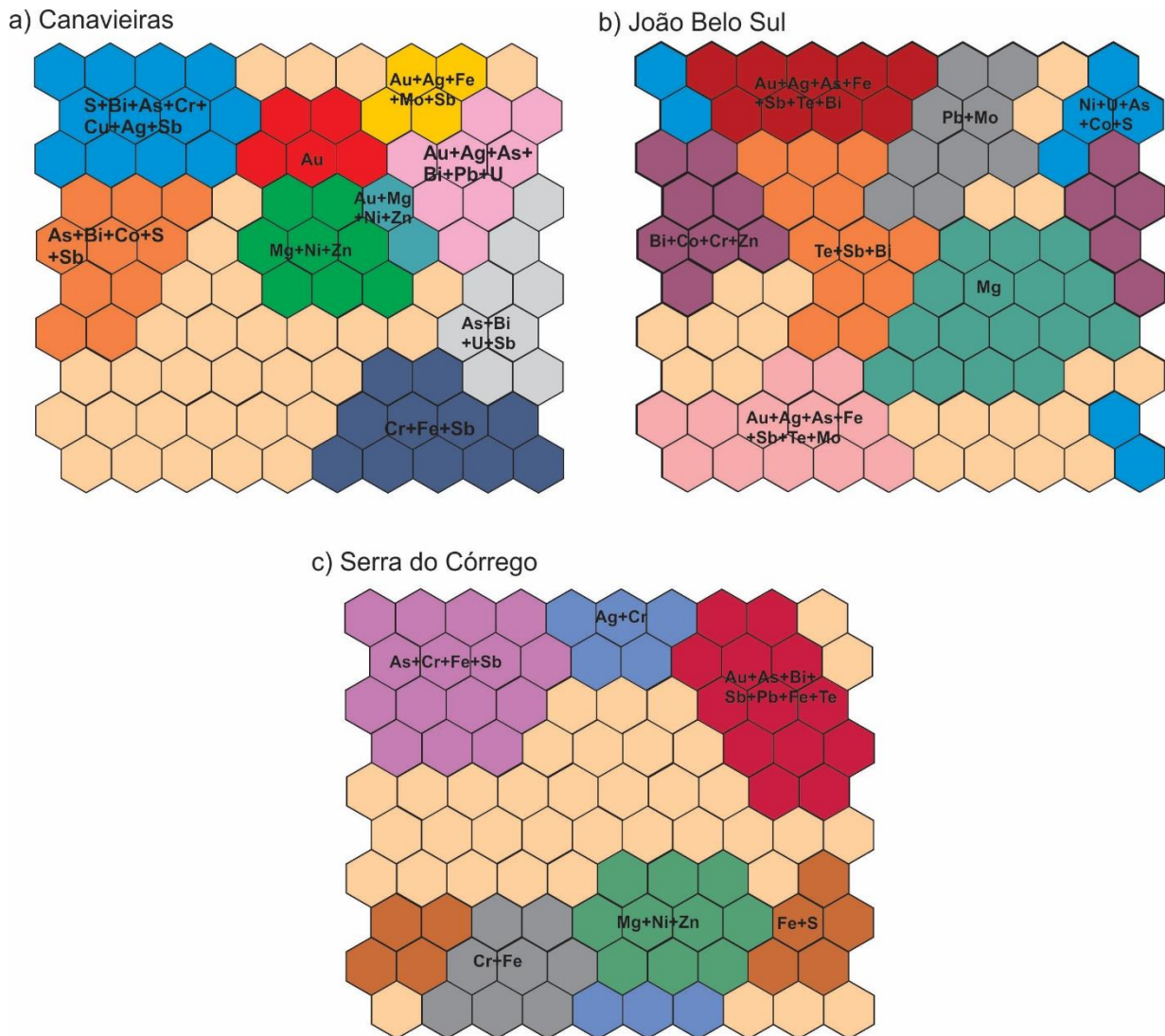


Fig. 2.11. Delineation of geochemical associations mapped in SOM for each of the targets. The elemental assemblages correlated to gold mineralization are described in table 2.6.

5. Discussion

5.1 Local geochemical background

Despite displaying similar petrographic characteristics, metaconglomerates from the Serra do Córrego Formation show distinct geochemical affinities. This behavior is explicitly evident in the PC1-PC2 diagram (Fig. 2.7), where metaconglomerate samples from each target cluster in three distinct directions. For João Belo Sul, the association of the metaconglomerate samples with chalcophile elements, Ag-U-As-Te-Bi-Sb-Pb, indicates an affinity with sulfide phases and the association with lithophile elements, Cr-Th-Sr-Hf-Zr-P, can indicate the relevance of depositional processes as these elements are enriched in the crust. In the Serra do Córrego target, the sample projections on the diagram indicates a correlation with Al-Na-Ti-K-Rb-Nb-Sc, the presence of alkalis – Na and K – can be related to the influence of hydrothermal fluids. Lastly, samples from Canavieiras show correlation with Ni-Fe-Mo-Mg-Mn-Li, probably related to mafic dykes that intensely intersect this target, and with Au-S-Co-Cu, which indicates an association with sulfide phases and gold mineralization.

From a prospective standpoint, understanding geochemical associations is crucial for the increased accuracy of exploration programs, especially in locations with a mature mining context like Jacobina. Despite being in a basin context, with evidence pointing to a common source for sediments (Milési et al., 2002; Pearson et al., 2005; Teles et al., 2015; Reis et al., 2021) and with mineralization predominantly confined to metaconglomerates, the mineralized bodies across the Jacobina mining district have shown different geochemical signatures. These differences are a result of combined factors that had different contributions along the basin, for example, deposition, hydrothermal alteration and gold remobilization related to late igneous mafic intrusions.

The petrographic results also contribute to the understanding of the geochemical background of the mineralized bodies in Jacobina. In the samples from the João Belo Sul target, the sedimentary pyrite phase is abundant. These pyrites are strongly oxidized, sometimes forming pseudomorphs with included gold (Fig. 2.5h). These petrographic characteristics, combined with the results of the PCA, suggest a greater similarity to paleoplacer-type deposits for the João Belo Sul target. However, the outcomes for Serra do Córrego and Canavieiras lean towards a hydrothermal mineral system delineated by the influence of fluids. This is evidenced by the PCA results for both targets, revealing

correlations with hydrothermal fluids and mafic-ultramafic dikes that intersect the unit. Additionally, this interpretation is supported by petrographic evidence, where in Canavieiras samples, epigenetic pyrites dominate, with the presence of sedimentary pyrite being less common. These distinct geochemical signatures for the mineralized bodies in the Jacobina Basin imply that different exploratory strategies need to be adopted, considering the specific characteristics of each target.

5.2 Unsupervised learning and the delineation of pathfinder element assemblages

The two employed unsupervised classification methodologies converge in the same direction: gold mineralization in the Serra do Córrego Formation is primarily associated with pyrites. Whether the origin of this mineralization is syngenetic or epigenetic, both PCA and SOM indicate correlations of Au with chalcophile elemental assemblages across the three studied targets. The identified correlations from each methodology are summarized in table 2.6.

Recent works by Teles et al. (2020) and Garayp and Frimmel (2023) had already proposed this significant relationship between gold and pyrites. Both studies characterize distinct types of pyrites: sedimentary pyrite and epigenetic pyrite. Using LA-ICPMS data, they show that sedimentary pyrite has the highest Au content and is enriched in other trace elements such as As, Ag, Pb, Te, and Bi, while the other two types are significantly depleted in these elements. The authors employ these geochemical evidences, along with petrographic and isotopic data, to support the modified paleoplacer model. From the perspective of Milési (2002) and Pearson (2005), they acknowledge the association of gold with pyrites and by LA-ICPMS they attest their enrichment in Ni, Co and V. However, for these authors, all pyrites are of hydrothermal origin, favoring the epigenetic model for gold mineralization in Jacobina.

Table. 2.6. Summarized geochemical signatures of gold mineralization identified by principal component analysis and self-organizing maps.

	Principal Component Analysis	Self-Organizing Maps
João Belo Sul	Au-As-Fe-S-Sb-U-Bi	Au-Ag-As-Fe-Sb-Te-Bi
	Au-Ag-Sr-Sb-Te-Pb-Mo	Au-Ag-As-Fe-Sb-Te-Mo
Canavieiras	Au-Cr-Fe-Th-Pb-Ag-Bi-Te-U-Mo	Au-Ag-Fe-Mo-Sb
		Au-Ag-As-Bi-Pb-U
	Mg-Zn-Ni-Ga-Ti-Sc	Au-Mg-Ni-Zn
		Au only
Serra do Córrego	Au-As-Te-Pb-U-Sr-Sb-Th-Bi	Au-As-Bi-Sb-Pb-Fe-Te

Our study does not aim to advocate for or against any of the proposed metallogenetic models for the Jacobina gold district. Regardless of the style of mineralization, our results point to a dominant association of mineralized metaconglomerates with pyrites. This relationship is marked by the positive correlation between Au and the elements Ag, As, Fe, Sb, Bi, Mo, Pb, and U, which occurs, with slight variations, in all three targets studied—João Belo Sul, Serra do Córrego, and Canavieiras.

PCA and SOM yield similar results for João Belo Sul and Serra do Córrego (Table 2.6). Considering that, for SOM, we removed some elements from our input data, we mapped the same geochemical signatures using each method. For João Belo Sul, the gold mineralization signature is marked by a chalcophile association of Au-Ag-As-Fe-Sb-Te-Bi and Au-Ag-As-Fe-Sb-Te-Mo. For Serra do Córrego, the mineralization footprint is also marked by a chalcophile association, Au-As-Bi-Sb-Pb-Fe-Te

Unlike João Belo Sul and Serra do Córrego, the data from the metaconglomerates of Canavieiras reveal that the gold mineralization in this area exhibits more than one geochemical signature. Initially, with PCA, we identified two groups of mineralized samples with distinct geochemical affinities (Fig. 2.8B). The first mapped geochemical correlation (Au-Cr-Fe-Th-Pb-Ag-Bi-Te-U-Mo) indicates the association of Au with elements found in pyrites, as previously reported by Teles et al. (2020) and Garayp and Frimmel (2023). However, in our study, a second group stands out and is identified by the concentration of mineralized samples plotted in the direction of eigenvectors indicating mafic affinities (Mg-Zn-Ni-Ga-Ti-Sc).

By the clustering of SOM component plots, we identified not only two but three distinct geochemical signatures for Canavieiras (Fig. 2.9a). The first signature, like the one for the other two targets, is the associated with gold found in pyrites, marked by the following element associations - Au-Ag-Fe-Mo-Sb and Au-Ag-As-Bi-Pb-U. Next, there is a small cluster marking the correlation between gold and mafic rocks (Au-Mg-Ni-Zn), similar to the one found with PCA. Lastly, with SOM, we identified a prominent cluster delineating a gold-only signature.

As mentioned previously, the Canavieiras mine stands out due to its significant contribution to gold production, as it concentrates the highest gold grades within the district. The significance of this mine is such that in 1968, Gross published the first paper with a detailed study of gold mineralization at the Canavieiras mine. Despite stating in that work, based on the information available at the time, that there was no evidence of a

direct relationship between gold and pyrites, Gross in 1968 had already mentioned a certain influence of mafic-ultramafic dikes and sills on gold remobilization. As well as the presence of free gold associated with veinlets, fractures, and faults in Canavieiras.

In the present day, we continue to seek an understanding of what sets this mine apart from other mines and exploratory targets in the Jacobina deposit. The influence of dikes and sills in Canavieiras is pervasive and much more pronounced than in other mines. These mafic-ultramafic bodies intersect all units of the Serra do Córrego Formation with different orientations and kinematics. In comparison to the João Belo Norte mine, for every 100,000 meters of drilling, Canavieiras has 3.5 times more meters intercepting these dikes and sills. While the precise ages of these mafic bodies remain undetermined, their likely emplacement coincided with the evolution of the basin, evidenced by their deformation and metamorphism during the Paleoproterozoic orogeny. The emplacement of these dykes in an unconsolidated basin would favor the interaction between the mafic magma and the mineralized metaconglomerates. A relationship that is evident by high grade mineralized zones in the contact between the metaconglomerates and the dykes.

Based on the results of unsupervised classification, we can confirm the significant contribution that mafic-ultramafic dikes and sills made to gold mineralization of metaconglomerates in Canavieiras. Regardless of the source of gold, there is evidence in Canavieiras indicating that fluids associated with this basic magmatism played a crucial role in gold solubilization, transport, and precipitation—a phenomenon not observed in the other two studied targets. Earlier studies have highlighted the presence of mafic-ultramafic bodies as the origin of Cr within the Jacobina Basin, identified in pyrites and fuchsite (Milési et al., 2002; Pearson, 2005, Teles et al., 2015; Teles et al., 2020; Garayp and Frimmel, 2023). These studies also report the occurrence of local gold-bearing mafic-ultramafic bodies. Here, we identified a signature Au-Mg-Ni-Zn in the mineralized metaconglomerates that is compatible with the influence of mafic rocks, and it is not correlated with Cr.

In their most recent article, Garayp and Frimmel (2023) conducted microprobe analyses on various gold grains. They identified a depletion of trace elements, particularly Ag, in gold located in veins compared to gold found in pyrites. The authors argue that the purification of gold through remobilization induced by post-depositional fluids is evident. For Canavieiras, we have clearly defined a cluster of free gold that we associate with this gold generation, occurring in veins, fractures, and faults. This geochemical signature

confirms the significant role of post-depositional fluids in the mineralization processes of Canavieiras mine.

The presence of three geochemical signatures, indicating the coexistence of distinct stages of mineralization, is certainly a contributing factor to Canavieiras having the highest grades of gold in the Jacobina district. This result perfectly aligns with the mineral system approach, as it illustrates how the combined influence of critical components determines the formation of an ore body, shaping its size and economic value (Megill, 1988).

Even though our results did not point to hydrothermal geochemical signatures for the gold mineralization in João Belo Sul and Serra do Córrego, that does not mean hydrothermal processes are not relevant all along the basin. There is evidence of the circulation of magmatic fluids throughout the entire Jacobina Range, and these are associated with the remobilization of gold in the system (Milesi et al. 2002; Teles et al. 2020; Miranda et al. 2021; Garayp and Frimmel 2023). In Garayp and Frimmel (2023) recent work, various gold occurrences were analyzed, and of these, about 20% occur in veins, microstructures, and fractures, being associated with remobilization. Most of their samples came from the Canavieiras domain, and comparing with the results obtained here, it can be considered that remobilized gold is less abundant in the other targets, and that could be why this correlation was not mapped by unsupervised classification.

6. Conclusions

The mapping of different geochemical signatures of gold mineralization in the upper metaconglomerates from the Jacobina basin constitutes a novel, unforeseen, and remarkable outcome. This underscores the crucial role of exploratory geochemistry, even in near-mine contexts. Exploratory analysis techniques applied to litho-geochemical data have demonstrated notable efficiency in expanding the scope of mineral exploration. By discerning and interpreting the chemical and mineral signals associated with economically valuable deposits, these methods contribute significantly to enlarging the target size for exploration.

Through unsupervised classification, we were able to identify distinct geochemical signatures for gold-mineralized bodies in the Jacobina mining district. Principal component analysis was initially applied to demonstrate that the upper metaconglomerates of the Serra do Córrego Formation exhibit different geochemical

affinities along the NS trend of the basin. Considering a common source for these rocks, the geochemical assemblage characteristic of each body is associated with the mineralizing process and the tectonic framework that acted differently across the Jacobina Basin. We have the following signatures for the upper metaconglomerates: (1) for João Belo Sul, elements with lithophile and chalcophile affinities, such as As, Te, Bi, Sb, Th, Hf, and Zr; (2) for Serra do Córrego, elements associated with hydrothermal fluids, such as Na, K, Al, Nb, and Sc; (3) for Canavieiras, elements of mafic origin and associated with gold mineralization, including Mg, Fe, Ni, S, Au, Co, and Cu.

In the second phase, we employed multivariate analysis and neural networks, specifically PCA and SOM, to characterize the geochemical signature of gold mineralization in the upper metaconglomerates of the Serra do Córrego Formation. Both methods reveal a strong correlation between gold mineralization and the presence of pyrites in the three studied targets. This relation can be visualized by the association of Au with elements such as Ag, As, Fe, Sb, Bi, Mo and Pb.

Apart from gold associated with pyrites, SOM identified two additional signatures for Canavieiras: (1) gold linked to mafic-ultramafic dikes and sills, characterized by the correlation between Au-Mg-Ni-Zn; (2) and free gold, which is depleted in trace elements and is associated to gold located in faults and fractures.

The delineation of these three mineralization phases coexisting in Canavieiras provides crucial insights into why it stands out as the mine with the highest average gold grade in the Jacobina district. It also sheds light on the significance of remobilization processes in the dynamics of the mineralizing system, contributing to the reconcentration of ore and the formation of high-grade zones.

In terms of method comparison, the achieved results were coherent and similar. PCA is a widely used method in the geosciences, easily applicable in mineral exploration routines for mapping prospective vectors. However, to extract the best from this tool, a good understanding of the geological context is necessary for the optimal selection of variables to be used in the input data. On the other hand, SOM is a more robust method, offering excellent visualization and enabling a deeper interpretation of data. Nevertheless, it requires a greater familiarity with machine learning algorithms.

Acknowledgments

The authors would like to thank Pan American Silver Corp. for providing data and financing this study. A special thanks to geologist Juliano José de Souza for the support, discussions and assistance facilitating the project. To geologist Guilherme Ferreira we

thank the suggestions and discussions related to multivariate analysis. We also would like to thank the entire exploration team from Jacobina, geologists, technicians and auxiliaries for all the help collecting the data. C.L.B. Toledo and A.M. Silva thank the Conselho Nacional de Desenvolvimento Científico e Tecnológico (CNPq) for their respective research grants. This study was financed in part by the Coordenação de Aperfeiçoamento de Pessoal de Nível Superior - Brasil (CAPES) - Finance Code 001.

7. References

Aitchison, J. (1982). The Statistical Analysis of Compositional Data. *Journal of the Royal Statistical Society: Series B (Methodological)*, 44(2), 139–160. <https://doi.org/10.1111/j.2517-6161.1982.tb01195.x>

Almeida, F. (1977). O cráton do São Francisco. *Revista Brasileira De Geociências*, 7:349–364.

Barbosa, J. (1997). Síntese Do Conhecimento Sobre A Evolução Geotectônica Das Rochas Metamórficas Arqueanas E Paleoproterozóicas Do Embasamento Do Craton Do São Francisco Na Bahia. In *Revista Brasileira de Geociências*.

Barbosa, J. S. F., & Sabaté, P. (2004). Archean and Paleoproterozoic crust of the São Francisco Craton, Bahia, Brazil: geodynamic features. *Precambrian Research*, 133(1–2), 1–27. <https://doi.org/10.1016/j.precamres.2004.03.001>

Bateman, J. D. (1958). Uranium-bearing auriferous reef at Jacobina, Brazil. *Economic Geology*, 53, 417–425.

Caté, A., Gloaguen, E., Blouin, M. (2017). Machine learning as a tool for geologists. *The Leading Edge*. 10.1190/tle36030064.1.

Chen, L. et al 2020 J. Phys.: Conf. Ser. 1684 012007

Chen, Z., Xiong, Y., Yin, B., Sun, S., & Zuo, R. (2023). Recognizing geochemical patterns related to mineralization using a self-organizing map. *Applied Geochemistry*, 151, 105621. <https://doi.org/10.1016/j.apgeochem.2023.105621>

Ferreira da Silva, G., Silva, A. M., Toledo, C. L. B., Chemale Junior, F., & Klein, E. L. (2022). Predicting mineralization and targeting exploration criteria based on machine-learning in the Serra de Jacobina quartz-pebble-metaconglomerate Au-(U) deposits, São Francisco Craton, Brazil. *Journal of South American Earth Sciences*, 116, 103815. <https://doi.org/10.1016/j.jsames.2022.103815>

Filzmoser, P., Hron, K. and Reimann, C. (2009) Univariate Statistical Analysis of Environmental (Compositional) Data: Problems and Possibilities. *Science of the Total Environment*, 407, 6100-6108. <http://dx.doi.org/10.1016/j.scitotenv.2009.08.008>

Frimmel, H. E., le Roex, A. P., Knight, J., & Minter, W. E. L. (1993). A case study of the postdepositional alteration of the Witwatersrand Basal Reef gold placer. *Economic Geology*, 88(2), 249–265. <https://doi.org/10.2113/gsecongeo.88.2.249>

Frimmel, H. E., Groves, D. I., Kirk, J., Ruiz, J., Chesley, J., & Minter, W. E. L. (2005). The Formation and Preservation of the Witwatersrand Goldfields, the World's Largest Gold Province. *Economic Geology, 100th Anniversary*, 769–797.

Frimmel, Hartwig. (2019). The Witwatersrand Basin and Its Gold Deposits: Methods and Protocols. 10.1007/978-3-319-78652-0_10.

Gaillard, N., Williams-Jones, A. E., Clark, J. R., Salvi, S., Perrouty, S., Linnen, R. L., & Olivo, G. R. (2020). The use of lithogeochemistry in delineating hydrothermal fluid pathways and vectoring towards gold mineralization in the Malartic district, Québec. *Ore Geology Reviews*.

Garayp, E., & Frimmel, H. E. (2023). A modified paleoplacer model for the metaconglomerate-hosted gold deposits at Jacobina, Brazil. *Mineralium Deposita*. <https://doi.org/10.1007/s00126-023-01220-9>

Gouvêa, R. C. T., Gioria, R. dos S., Marques, G. R., & Carneiro, C. de C. (2023). IntraSOM: A comprehensive Python library for Self-Organizing Maps with hexagonal toroidal maps training and missing data handling. *Software Impacts*, 17, 100570. <https://doi.org/10.1016/j.simpa.2023.100570>

Gross, W. H. (1968). Evidence for a Modified Placer Origin for Auriferous Conglomerates, Canavieiras Mine, Jacobina, Brazil. In *Economic Geology* (Vol. 63).

Groves, D. I., Santosh, M., & Zhang, L. (2020). A scale-integrated exploration model for orogenic gold deposits based on a mineral system approach. *Geoscience Frontiers*, 11(3), 719–738. <https://doi.org/10.1016/j.gsf.2019.12.007>

Grunsky, E. C. (2010). The interpretation of geochemical survey data. *Geochemistry: Exploration, Environment, Analysis*, 10(1), 27–74. <https://doi.org/10.1144/1467-7873/09-210>

Hood, S. B., Cracknell, M. J., Gazley, M. F., & Reading, A. M. (2019). Element mobility and spatial zonation associated with the Archean Hamlet orogenic Au deposit, Western Australia: Implications for fluid pathways in shear zones. *Chemical Geology*, 514, 10–26. <https://doi.org/10.1016/j.chemgeo.2019.03.022>

Jolliffe, I. T., & Cadima, J. (2016). Principal component analysis: a review and recent developments. *Philosophical Transactions of the Royal Society A: Mathematical*,

Physical and Engineering Sciences, 374(2065), 20150202.
<https://doi.org/10.1098/rsta.2015.0202>

Kohonen, T. (1990). The self-organizing map. *Proceedings of the IEEE*, 78(9), 1464–1480. <https://doi.org/10.1109/5.58325>

Kohonen, T. (1997). *Self-Organizing Maps* (Vol. 30). Springer Berlin Heidelberg. <https://doi.org/10.1007/978-3-642-97966-8>

Kohonen, T. (2013). Essentials of the self-organizing map. *Neural Networks*, 37, 52–65. <https://doi.org/10.1016/j.neunet.2012.09.018>

Ledru, P., Milési, J. P., Johan, V., Sabate', P., & Maluski, H. (1997). Foreland basins and gold-bearing conglomerates: a new model for the Jacobina Basin (São Francisco province, Brazil). *Precambrian Research*, 86(3–4), 155–176. [https://doi.org/10.1016/S0301-9268\(97\)00048-X](https://doi.org/10.1016/S0301-9268(97)00048-X)

Leite, C.M.M. A evolução geodinâmica da orogênese paleoproterozóica nas regiões de Capim Grosso - Jacobian e Pintadas - Mundo Novo (Bahia, Brasil): Metamorfismo, anatexia crustal e tectônica. 2002. 412 f. Tese (Thesis) - Instituto de Geociências, Universidade Federal da Bahia

Leite, C., Barbosa, J., Nicollet, C., & Sabaté, P. (2007). Evolução metamórfica/metassomática Paleoproterozóica do Complexo Saúde, da Bacia de Jacobina e de leucogranitos peraluminosos na parte norte do Cráton do São Francisco. *Revista Brasileira De Geociências*, 37, 777–797.

Leite, C., & Marinho, M. (2012). Serra de Jacobina e Contendas-Mirante. In: BARBOSA, J.S.F. (Coord.). *Geologia da Bahia: pesquisa e atualização*. Salvador: CBPM, 2012. v.1, p. 397-441.

Leo, G., Cox, D., & Carvalho, J. (1964). Geologia da Parte Sul da Serra de Jacobina, Bahia, Brasil. *DNPM Boletim*, 209, 87.

Mascarenhas JF, Conceição Filho VM, Griffon JC (1992) Contribuição à geologia do Grupo Jacobina, região Jacobina/Pindobaçu. Congresso Brasileiro De Geologia Boletim De Resumos Expandidos SBG Brasil 2:141–142

Liu, Y. (2023). Machine Learning in Geology: Challenges and Prospects. *Highlights in Science, Engineering and Technology*. 44. 14-21. [10.54097/hset.v44i.7162](https://doi.org/10.54097/hset.v44i.7162).

Megill, R.E. (1988). *Exploration Economics*. PennWell, Tulsa, p.238.

Mccuaig, T. C., Beresford, S., & Hronsky, J. (2010). Translating the mineral systems approach into an effective exploration targeting system. *Ore Geology Reviews*, 38(3), 128–138. <https://doi.org/10.1016/j.oregeorev.2010.05.008>

Milesi, J. P., Ledru, P., Marcoux, E., Mougeot, R., Johan, V., Lerouge, C., Sabaté, P., Bailly, L., Respaut, J. P., & Skipwith, P. (2002). The Jacobina Paleoproterozoic gold-bearing conglomerates, Bahia, Brazil: a “hydrothermal shear-reservoir” model. *Ore Geology Reviews*, 95–136. www.elsevier.com/locate/oregeorev

Miranda, D. A., Misi, A., Klein, E. L., Castro, M. P., & Queiroga, G. (2021). A mineral system approach on the Paleoproterozoic Au-bearing quartz veins of the Jacobina Range, northeastern of the São Francisco Craton, Brazil. *Journal of South American Earth Sciences*, 106, 103080. <https://doi.org/10.1016/j.jsames.2020.103080>

Pearson WN, Macedo P M, Rubio A, Lorenzo C L, Karpeta P (2005). Geology and gold mineralization of the Jacobina Mine and Bahia Gold Belt, Bahia, Brazil, and a comparison to Tarkwa and Witwatersrand. Window to the World: 2005 Symposium Proceedings Geological Society of Nevada, Reno/Sparks Nevada, pp 757–785

Reis, C et al. (2021). Projeto Integração Geológica E Avaliação Do Potencial Metalogenético Da Serra De Jacobina E Do Greenstone Belt Mundo Novo. Informe de Recursos Minerais, Série Províncias Minerais do Brasil 31 CPRM pp 169. <https://doi.org/10.1111/j.1365-3121.2007.00764.x>

Robb, L. J., & Mayer, F. M. (1991). A contribution to recent debate concerning epigenetic versus syngenetic mineralization processes in the Witwatersrand basin. *Economic Geology*, 86, 396–401.

Sabaté, P., Marinho, M. M., Vidal, P., & Caen-Vachette, M. (1990). The 2-Ga peraluminous magmatism of the Jacobina-Contendas Mirante belts (Bahia, Brazil): Geologic and isotopic constraints on the sources. *Chemical Geology*, 83(3–4), 325–338. [https://doi.org/10.1016/0009-2541\(90\)90288-I](https://doi.org/10.1016/0009-2541(90)90288-I)

Santos, F. P., Chemale Junior, F., & Meneses, A. R. A. S. (2019). The nature of the Paleoproterozoic orogen in the Jacobina Range and adjacent areas, northern São Francisco Craton, Brazil, based on structural geology and gravimetric modeling. *Precambrian Research*, 332, 105391. <https://doi.org/10.1016/j.precamres.2019.105391>

Teixeira, J. B. G., de Souza, J. A. B., da Silva, M. D. G., Leite, C. M. M., Barbosa, J. S. F., Coelho, C. E. S., Abram, M. B., Filho, V. M. C., & Iyer, S. S. S. (2001). Gold mineralization in the Serra de Jacobina region, Bahia Brazil: Tectonic framework and metallogenesis. *Mineralium Deposita*, 36(3–4), 332–344. <https://doi.org/10.1007/s001260100174>

Teles, G., Chemale, F., & de Oliveira, C. G. (2015). Paleoproterozoic record of the detrital pyrite-bearing, Jacobina Au-U deposits, Bahia, Brazil. *Precambrian Research*, 256, 289–313. <https://doi.org/10.1016/j.precamres.2014.11.004>

Teles, G. S., Chemale, F., Ávila, J. N., Ireland, T. R., Dias, A. N. C., Cruz, D. C. F., & Constantino, C. J. L. (2020). Textural and geochemical investigation of pyrite in Jacobina Basin, São Francisco Craton, Brazil: Implications for paleoenvironmental conditions and formation of pre-GOE metaconglomerate-hosted Au-(U) deposits. *Geochimica et Cosmochimica Acta*, 273, 331–353. <https://doi.org/10.1016/j.gca.2020.01.035>

Vesanto, J., & Alhoniemi, E. (2000). Clustering of the self-organizing map. *IEEE Transactions on Neural Networks*, 11(3), 586–600. <https://doi.org/10.1109/72.846731>

Wafforn, M., Delgado, A., Andrews, M., Passos, C., Iturralde, C. (2023) NI 43-101 Technical Report for the Jacobina Gold Mine, Bahia State, Brazil. Pan American Silver Corp.

Wyborn, L.A., Heinrich, C.A., Jaques, A.L., 1994. Australian proterozoic mineral systems essential ingredients and mappable criteria. AusIMM Public.pp. 109–115.

Zuo, R. (2011). Identifying geochemical anomalies associated with Cu and Pb–Zn skarn mineralization using principal component analysis and spectrum–area fractal modeling in the Gangdese Belt, Tibet (China). *Journal of Geochemical Exploration*, 111(1–2), 13–22. <https://doi.org/10.1016/j.gexplo.2011.06.012>

Zuo, R., Xia, Q., Wang, H., 2013. Compositional data analysis in the study of integrated geochemical anomalies associated with mineralization. *Appl. Geochem.* 28, 202–211.

Zuo, R., Wang, J., Xiong, Y., & Wang, Z. (2021). The processing methods of geochemical exploration data: past, present, and future. *Applied Geochemistry*, 132, 105072. <https://doi.org/10.1016/j.apgeochem.2021.105072>

Capítulo 3

1. Considerações finais

Os resultados alcançados nessa pesquisa a partir da aplicação de algoritmos de *machine learning* permitiram caracterizar as assinaturas geoquímicas dos metaconglomerados e da mineralização de ouro no distrito de Jacobina. Além disso, foi feito um trabalho comparativo entre as metodologias de análise multivariada e redes neurais que retornou resultados similares e coerentes dentro do contexto geológico da área.

Inicialmente por meio da análise do componente principal foi possível reconhecer diferentes afinidades geoquímicas nas amostras de metaconglomerado dos três alvos estudado: João Belo Sul, Serra do Córrego e Canavieiras. Todas as amostras são da unidade superior da Formação Serra do Córrego e a partir do PCA é possível reconhecer as seguintes assinaturas geoquímicas: (1) crustal e calcófila para as rochas do alvo João Belo Sul, marcada pelos elementos U, As, Te, Bi, Sb, Pb, Cr, Th, Sr, Hf, Zr e P; (2) hidrotermal nos metaconglomerados do Serra do Córrego, indicada pela afinidade com Al, Na, Ti, Rb, K, Nb, e Sc; (3) máfica e aurífera para Canavieiras, pela correlação com os elementos Z, Cu, Co, S, Au, Ni, Fe, Mo, Li, Mg, e Mn.

Os sedimentos que compõem a Formação Serra do Córrego são interpretados oriundos de uma mesma fonte. O trabalho de Teles et al. (2015) conclui que o material que preenche a Bacia de Jacobina tem como única fonte as rochas TTG-greenstone do Bloco Gavião (3.2- 3.5Ga). Por esse motivo, tanto na produção científica quanto no meio industrial nunca foi considerado que os diferentes corpos mineralizados no complexo de Jacobina apresentariam afinidades geoquímicas distintas.

Nesse contexto, é possível que as distintas assinaturas geoquímicas mapeadas resultem da complexidade do sistema mineral, da disposição dos corpos ao longo da bacia e do arcabouço estrutural, favorecendo a migração de fluidos em áreas específicas. Do ponto de vista prospectivo, essa descoberta inicial indica que, para o João Belo Sul, a quantificação e caracterização das fases sulfetadas são de maior importância, enquanto, para Canavieiras e Serra do Córrego, compreender os controles estruturais e mapear possíveis condutos dos fluidos pós-deposicionais pode ser mais relevante.

Na segunda etapa desse trabalho realizamos uma comparação entre a aplicação de análise do componente principal e os mapas auto-organizáveis para caracterizar a assinatura geoquímica da mineralização de ouro nesses mesmos três alvos. Concluímos

que a maior parte da mineralização de ouro nos metaconglomerados da Formação Serra do Córrego é associada a piritas, essa relação é marcada por associações de Au com elementos como Ag, As, Fe, Sb, Bi, Mo e Pb que ocorrem nos três alvos. No entanto, para Canavieiras fica evidente outras duas assinaturas da mineralização, o ouro associado aos corpos máficos-ultramáficos, indicado pela associação Au-Mg-Ni-Zn, e o ouro livre.

Sendo Canavieiras o alvo de maior teor de ouro no complexo mineiro de Jacobina, concluímos que essa condição é resultado do acúmulo de três fases de mineralização distintas, o que não é mapeado nos outros corpos estudados. Tem-se para Canavieiras um grande exemplo da eficácia de um sistema mineral, no qual a sobreposição de diferentes eventos mineralizantes juntamente com fluxo de fluidos hidrotermais contribuiu para maior concentração de ouro. Os resultados alcançados nessa pesquisa vão de encontro ao proposto por Teles et al. (2020) e Garayp e Frimmel (2023). Os autores mostram que o maior conteúdo de ouro está nas piritas, mas identificam uma fase de ouro livre fortemente depletada em elementos-traço. Garayp e Frimmel (2023) inclusive abordam sobre a purificação do ouro a partir da remobilização por fluidos pós-deposicionais.

O objetivo proposto inicialmente para o trabalho foi alcançado, o emprego das metodologias de classificação não supervisionada foi bastante eficaz na caracterização do *footprint* geoquímico do complexo de Jacobina. Abaixo seguem algumas considerações e reflexões obtidas após a conclusão deste trabalho:

- (1) Num contexto de exploração mineral onde não é comum ter especialistas das diferentes áreas das geociências, as equipes costumam ser formadas por profissionais que tenham o mínimo de afinidade com diversos tópicos, como geologia estrutural, geoquímica e geofísica. Nesse cenário, o PCA é um método mais universal e que provou alcançar resultados coerentes podendo facilmente ser incorporado na rotina da exploração. O SOM é um método mais robusto e que explorou mais o banco de dados, porém, exige um conhecimento e habilidades maiores com algoritmos de machine learning.
- (2) A partir desse trabalho foram mapeadas algumas particularidades da geologia e da mineralização de cada alvo. Entender que existem estilos diferentes de mineralização ao longo da Bacia de Jacobina e introduzir essas particularidades como critérios na elaboração dos programas exploratórios aumenta a chance de atingir interceptos positivos.

- (3) As paragêneses elementares farejadoras da mineralização podem ser utilizadas na elaboração de um modelo geoquímico 3D em software como o Leapfrog Geo. A partir de um modelo que indique zonas enriquecidas nesses elementos é possível o mapeamento de zonas favoráveis a mineralização.
- (4) Ampliar os investimentos e inserir na rotina a caracterização geoquímica das amostras, seja amostra de furos de sondagem ou amostras de superfície é fundamental para a continuidade dos programas exploratórios. O trabalho realizado por Bluemel (2021) no depósito tipo *placer* de Castelo dos Sonhos, estado do Pará, possibilitou um aumento significativo do recurso mineral da empresa após a aplicação de uma rotina de análise litogeoquímica seguida de mapeamento de padrões geoquímicos com o PCA.

2. Referências bibliográficas

Bluemel, B. (2021) What Can Machine Learning Do for Me? Improved Targeting, 3D Modelling, and Resource Estimation: A Case Study from the Castelo do Sonhos Paleoplacer Gold Deposit, Brazil. SEG 100 Conference. Whistler, BC, Canada.

Garayp, E., & Frimmel, H. E. (2023). A modified paleoplacer model for the metaconglomerate-hosted gold deposits at Jacobina, Brazil. *Mineralium Deposita*. <https://doi.org/10.1007/s00126-023-01220-9>

Teles, G., Chemale, F., & de Oliveira, C. G. (2015). Paleoproterozoic record of the detrital pyrite-bearing, Jacobina Au-U deposits, Bahia, Brazil. *Precambrian Research*, 256, 289–313. <https://doi.org/10.1016/j.precamres.2014.11.004>

Teles, G. S., Chemale, F., Ávila, J. N., Ireland, T. R., Dias, A. N. C., Cruz, D. C. F., & Constantino, C. J. L. (2020). Textural and geochemical investigation of pyrite in Jacobina Basin, São Francisco Craton, Brazil: Implications for paleoenvironmental conditions and formation of pre-GOE metaconglomerate-hosted Au-(U) deposits. *Geochimica et Cosmochimica Acta*, 273, 331–353. <https://doi.org/10.1016/j.gca.2020.01.035>